



HAL
open science

5-HT1A and 5-HT2B receptor interaction and co-clustering regulate serotonergic neuron excitability

Amina Benhadda, Célia Delhayé, Imane Moutkine, Xavier Marques, Marion Russeau, Corentin Le Magueresse, Anne Roumier, Sabine Lévi, Luc Maroteaux

► **To cite this version:**

Amina Benhadda, Célia Delhayé, Imane Moutkine, Xavier Marques, Marion Russeau, et al.. 5-HT1A and 5-HT2B receptor interaction and co-clustering regulate serotonergic neuron excitability. *iScience*, 2023, 26 (8), pp.107401. 10.1016/j.isci.2023.107401 . hal-04196168

HAL Id: hal-04196168

<https://hal.science/hal-04196168>

Submitted on 5 Sep 2023

HAL is a multi-disciplinary open access archive for the deposit and dissemination of scientific research documents, whether they are published or not. The documents may come from teaching and research institutions in France or abroad, or from public or private research centers.

L'archive ouverte pluridisciplinaire **HAL**, est destinée au dépôt et à la diffusion de documents scientifiques de niveau recherche, publiés ou non, émanant des établissements d'enseignement et de recherche français ou étrangers, des laboratoires publics ou privés.

5-HT1A and 5-HT2B receptor interaction and co-clustering regulate serotonergic neuron excitability
--Manuscript Draft--

Manuscript Number:	ISCIENCE-D-23-01784R4
Full Title:	5-HT1A and 5-HT2B receptor interaction and co-clustering regulate serotonergic neuron excitability
Article Type:	Research Article
Corresponding Author:	Luc Maroteaux Paris, FRANCE
First Author:	Amina Benhadda
Order of Authors:	Amina Benhadda Célia Delhaye Imane Moutkine Xavier Marques Marion Russeau Corentin Le Magueresse Anne Roumier Sabine Levi Luc Maroteaux
Abstract:	Many psychiatric diseases have been associated with serotonin (5-HT) neuron dysfunction. The firing of 5-HT neurons is known to be under 5-HT1A receptor-mediated autoinhibition, but functional consequences of coexpressed receptors are unknown. Using co-immunoprecipitation, BRET, confocal and super-resolution microscopy in hippocampal and 5-HT neurons, we present evidence that 5-HT1A and 5-HT2B receptors can form heterodimers and co-cluster at the plasma membrane of dendrites. Selective agonist stimulation of coexpressed 5-HT1A and 5-HT2B receptors prevents 5-HT1A receptor internalization and increases 5-HT2B receptor membrane clustering. Current clamp recordings of 5-HT neurons revealed that 5-HT1A receptor stimulation of acute slices from mice lacking 5-HT2B receptors in 5-HT neurons increased their firing activity through Ca ²⁺ -activated potassium channel inhibition compared to 5-HT neurons from control mice. This work supports the hypothesis that the relative expression of 5-HT1A and 5-HT2B receptors tunes the neuronal excitability of serotonergic neurons through potassium channel regulation.
Additional Information:	
Question	Response
Standardized datasets A list of datatypes considered standardized under Cell Press policy is available here . Does this manuscript report new standardized datasets?	No
Original code Does this manuscript report original code?	No

Manuscript ISCIENCE-D-23-01784R2

Dear editor,

Please find our second revision of our research manuscript entitled "**5-HT_{1A} and 5-HT_{2B} receptor interaction and co-clustering regulate serotonergic neuron excitability**" by Benhadda et al.

- We have included the STAR Methods text within the main article file, not the supplemental PDF.
- We have upload the completed KRT in Word format.
- We have added, a one-sentence descriptive title after the STAR Methods section for the Table S1 and removed this table from the supplemental PDF.
- We have uploaded a single Word document that includes four Highlights of no more than 89 characters, including spaces.
- We added "STAR Methods" , "Resource Availability"; The Data and Code Availability Section (which is not relevant to our manuscript); The "Any additional information ..."; Experimental Model and Subject Details section ; Method Details section; Quantification and Statistical Analysis .
- For "RNAseq" we provide the link in the manuscript.
- We completed the Key Resources Table.

Hoping that this revised manuscript is now suitable for publiaction, with my best regards,

Luc Maroteaux PhD

Manuscript Number: ISCIENCE-D-23-01784R2

"5-HT1A and 5-HT2B receptor interaction and co-clustering regulate serotonergic neuron excitability" by Benhadda et al.

We thank the reviewers for their positive comments and constructive advices to improve the manuscript. Please find below the answers to their concerns:

Reviewer #2:

Figure 2B,D,E: If you put a color legend under the graphs, remove the redundant legend under each bar for a clearer understanding

We have removed the redundant legend under each bars from Fig2B,D,E

Figure 3B: Put the same color legend under the graph and remove the bar title on x axis from underneath the graph like you did for the rest of the figure

We changed Fig 3B accoringly to the rest of the figure

Figure 4B: Remove the RS of "5-HT2B-R" for consistency between the figures in the legend

We removed 5-HT2B-R from fig 4B and from other figures (microscopy panels).

Figure 5B: Put the two colored squared of the "5-HT2B+5-HT1A" legend on one line like the others and Figure 7B: Same comment for the bar graph legend.

We put the two colored squared of the "5-HT2B+5-HT1A" legend on a single line in fig 5B and changed the bar graph legend of Fig7B

5-HT_{1A} and 5-HT_{2B} receptor interaction and co-clustering regulate serotonergic neuron excitability.

5-HT receptor cross-talks shape 5-HT neuron activity

Amina Benhadda, Célia Delhaye, Imane Moutkine, Xavier Marques, Marion Russeau, Corentin Le Magueresse, Anne Roumier, Sabine Lévi, and Luc Maroteaux¹

Institut du Fer à Moulin, U1270 INSERM, Sorbonne Université, 17 rue du Fer à Moulin 75005, Paris, France

Corresponding author: Luc Maroteaux, Email: luc.maroteaux@upmc.fr

SUMMARY

Many psychiatric diseases have been associated with serotonin (5-HT) neuron dysfunction. The firing of 5-HT neurons is known to be under 5-HT_{1A} receptor-mediated autoinhibition, but functional consequences of coexpressed receptors are unknown. Using co-immunoprecipitation, BRET, confocal and super-resolution microscopy in hippocampal and 5-HT neurons, we present evidence that 5-HT_{1A} and 5-HT_{2B} receptors can form heterodimers and co-cluster at the plasma membrane of dendrites. Selective agonist stimulation of coexpressed 5-HT_{1A} and 5-HT_{2B} receptors prevents 5-HT_{1A} receptor internalization and increases 5-HT_{2B} receptor membrane clustering. Current clamp recordings of 5-HT neurons revealed that 5-HT_{1A} receptor stimulation of acute slices from mice lacking 5-HT_{2B} receptors in 5-HT neurons increased their firing activity through Ca²⁺-activated potassium channel inhibition compared to 5-HT neurons from control mice. This work supports the hypothesis that the relative expression of 5-HT_{1A} and 5-HT_{2B} receptors tunes the neuronal excitability of serotonergic neurons through potassium channel regulation.

¹ Lead contact Luc Maroteaux, Email: luc.maroteaux@upmc.fr

INTRODUCTION

Many psychiatric diseases including depression, schizophrenia or anxiety have been associated with serotonin (5-HT) neuron activity dysfunctions¹⁻³. Dorsal raphe serotonin neurons (DR) and their long-range projections exert control over many physiological functions such as emotion, sleep and locomotion. Pacemaker-like firing of raphe 5-HT neurons was reported to be under 5-HT_{1A} receptor (5-HT_{1A})-mediated autoinhibition, although 5-HT neurons can also express other 5-HT receptors. With the exception of 5-HT₃ receptors, which are ion channels, all 5-HT receptors are G-protein coupled receptors (GPCR) that differ according to their G-protein coupling.

The 5-HT₁ subtypes are typically coupled to the G_{ai/o} protein and their activation may lead to a decrease in intracellular cAMP level⁴ among many other possible coupling depending on the cellular context⁵. In the central nervous system, 5-HT_{1A} functions as an autoreceptor, i.e. is expressed by 5-HT neurons themselves, in the raphe nuclei, and as heteroreceptors in neurons of several brain structures including hippocampus and prefrontal cortex⁵⁻⁷. In 5-HT neurons, 5-HT_{1A} are located to the somatodendritic compartment⁸. Through the G $\beta\gamma$ subunit, 5-HT_{1A} activation can induce the opening of potassium channels (G protein-coupled inwardly-rectifying potassium channels or GIRKs) which tends to hyperpolarize neurons⁹⁻¹². The tone of 5-HT neurons has thus been considered to be negatively regulated by 5-HT_{1A} autoreceptors expressed on their soma and dendrites in the raphe nuclei¹¹. Most serotonergic neurons have two key electrophysiological characteristics: a long-duration action potential and a prominent medium-duration afterhyperpolarization (mAHP), which plays a critical role in setting the firing frequency by delaying the occurrence of the next action potential.¹³ This mAHP is due to the opening of small-conductance Ca²⁺-activated potassium (SK) channels. Blockade of SK channels by apamin, a neurotoxin from bee venom, which is a potent antagonist of SK2 and SK3 subtypes, has been shown to increase 5-HT neuron burst firing (repeated action potentials separated by a small interval) in DR and extracellular 5-HT levels¹⁴ via a direct action¹⁵. It has been proposed that 5-HT_{1A} may also regulate SK channels¹⁶, in addition to GIRKs. Accumulating evidence indicate additional roles for 5-HT_{1A} in dorsal raphe beyond an homeostatic control of firing rate⁶. In particular, the 5-HT_{1A} autoreceptors internalization, which results in its desensitization¹⁷ is thought to participate to the delayed antidepressant effects of serotonin-specific reuptake inhibitors (SSRIs). Nevertheless, there is evidence that 5-HT_{1A}-dependent feedback inhibition of 5-HT neurons persists after sustained chronic exposure to high extracellular 5-HT as upon exposure to SSRIs¹⁸. Therefore, we asked if 5-HT_{1A} could interact with other 5-HT receptors to participate to the regulation of 5-HT neuron firing.

The 5-HT₂ receptor subtypes (5-HT_{2A}, _{2B}, _{2C}) are coupled to the G $\alpha_q/11$ protein that mainly activate phospholipase C (PLC) and increase inositol triphosphate (IP3) and Ca²⁺ intracellular concentration. A loss of function of *HTR2B*, the gene encoding 5-HT_{2B}, is associated with impulsivity, a higher risk of developing depression and suicidal behavior^{19,20}. Using behavioral and biochemical experiments in mice, Diaz et al.²¹ showed that 5-HT_{2B} is expressed in serotonergic neurons, which is confirmed by recent RNAseq^{22,23} (see https://bokaty.shinyapps.io/DR_Pet1_neuron_scRNAseq_DB/). The acute or chronic activation of 5-HT_{2B} by the preferential agonist BW723C86 (BW) can mimic SSRI effects in mice²¹. Accordingly, behavioral and molecular responses to SSRIs are abolished in mice lacking the 5-HT_{2B} specifically in 5-HT neurons (2B-KO^{5-HT} mice). Moreover, in WT mice, the activation of 5-HT_{2B} by BW is able to counteract the effects of 5-HT_{1A} autoreceptor activation by the selective agonist 8-hydroxy-2-(di-n-propylamino)tetralin (8-OHDPAT), such as the decrease in 5-HT neurons firing rate and in body temperature²⁴. Although 5-HT₂ signaling has been shown to crosstalk with 5-HT_{1A}²⁵, and 5-HT_{2B} are expressed by

serotonergic neurons together with 5-HT_{1A}²¹, interactions between these receptors and their putative consequence to serotonergic tone regulation are not yet documented.

The aim of this work was thus to test the hypothesis that interactions between 5-HT_{2B} and 5-HT_{1A} affect their impact on 5-HT neurons activity. By studying different models (COS-7 cells, primary cultures of hippocampal neurons, and raphe 5-HT neurons) with pharmacological, electrophysiological, and high-resolution imaging techniques, we show that 5-HT_{2B} and 5-HT_{1A} can form heterodimers. Moreover, coexpression of both receptors has no apparent effect on their respective ligand binding properties and their classical second messenger signaling, but alters their plasma membrane expression (local accumulation as clusters, cell membrane expression) during responses to specific ligands. Last, *ex-vivo* experiments reveal that their crosstalk affects the excitability of 5-HT neurons through SK and GIRK channels regulation.

RESULTS

Coexpression of 5-HT_{2B} with 5-HT_{1A} reveals direct interactions- We previously showed that 5-HT_{2B} and 5-HT_{1A} can be coexpressed in 5-HT neurons²¹ and have opposite actions on 5-HT neuronal activity²⁴. GPCRs including 5-HT receptors are able to form homo or heterodimers with each other or with non-5-HT receptors that modify their respective signaling pathways²⁶. To assess putative 5-HT_{2B} and 5-HT_{1A} interactions, we first performed co-immunoprecipitation experiments in COS-7 cells transfected with plasmids encoding HA-tagged 5-HT_{2B} and/or Myc-tagged 5-HT_{1A} (See STAR Methods). Immunoprecipitation of 5-HT_{2B} with anti-HA beads followed by Western blotting with anti-Myc antibody to assess the presence of 5-HT_{1A} revealed co-immunoprecipitation of 5-HT_{1A} with 5-HT_{2B} in cotransfected cells (**Fig. 1A**). We completed these data by performing BRET experiments to assess close vicinity of 5-HT_{1A} and 5-HT_{2B}. This experiment relies on the natural capacity of Renilla luciferase, used here as BRET donor, to emit energy in presence of its substrate, coelenterazine or to transfer it to an acceptor. The sequences of Luciferase (the BRET donor) and of yellow fluorescent protein (YFP, the BRET acceptor) were fused to the C-terminal coding region of 5-HT_{1A} and 5-HT_{2B}, respectively (See STAR Methods). Increasing amounts of BRET acceptor plasmids were co-transfected with a constant amount of BRET donor plasmid in COS-7 cells. A hyperbolic curve indicates saturation and thus specific interaction between the BRET donor and the acceptor and thus, the close proximity between the two proteins that carry them. Here, a hyperbolic curve was obtained when 5-HT_{2B} and 5-HT_{1A} were expressed together, supporting the hypothesis that they can form heterodimers in intact cells (**Fig. 1B**). As control, no BRET signal was obtained when 5-HT_{2B} was tested for self-association, confirming a previous study indicating that this receptor is unable to form homodimers²⁷. Thus, co-immunoprecipitation and BRET experiments revealed that 5-HT_{1A} and 5-HT_{2B} can interact closely and may form heteromers.

Total receptor expression and coupling to second messenger are not affected by 5-HT_{2B}/5-HT_{1A} coexpression- We assessed if coexpression of 5-HT_{1A} and 5-HT_{2B} affect their respective intracellular signaling pathway, and pharmacological properties. To this aim, we transfected COS-7 cells to express 5-HT_{2B} and/or 5-HT_{1A}, either alone or together, and prepared whole membrane protein extracts. We then performed radioligand binding competition assays for 5-HT_{2B} and 5-HT_{1A} in the different transfection conditions, to assess their B_{max}, which represents the total number of receptors available, and their K_i, which represents the affinity, for their specific ligand (See STAR Methods). No difference was found in B_{max} (not illustrated), nor in binding affinity (K_i) to their respective ligand, in coexpressing compared to single receptor expressing cells (**Fig. 1C-F**). The K_i of 5-HT_{2B} for its specific ligand BW was not affected by the coexpression of 5-HT_{1A} (**Fig. 1D**). Similarly, the K_i of 5-HT_{1A} for its specific ligand NAN was not affected by the coexpression of 5-HT_{2B} (**Fig. 1F**). This indicates that even if 5-HT_{1A} and 5-HT_{2B} can form heterodimers, as indicated by coIP and BRET experiments, this doesn't significantly change their affinity for ligands. Then, using HTRF-based assays, we measured the intracellular inositolphosphate (IP) amount produced by agonist stimulation of 5-HT_{2B}, in cells expressing both 5-HT_{2B} and 5-HT_{1A} or 5-HT_{2B} alone. IP measurement is a readout of the activation of Gq/PLC/IP₃ pathway, which is the classical downstream signaling of 5-HT_{2B} (See STAR Methods). The dose-response curve of IP production in response to increasing doses of BW, a specific agonist of 5-HT_{2B}, were analyzed using the operational model to determine the G_{aq} coupling efficiency of the receptor either alone or expressed together with 5-HT_{1A}. This showed that there was no significant difference in the EC₅₀ between the two conditions (**Fig. 1G-H**). These results indicate that 5-HT_{1A} and 5-HT_{2B} coexpression modifies neither their total expression level, nor their ligand binding, nor the G_{aq}/11 coupling efficiency of 5-HT_{2B}.

Coexpression of 5-HT_{2B} with 5-HT_{1A} decreases 5-HT_{2B} membrane expression- Trafficking of GPCRs to the plasma membrane is a process which can be regulated, notably by the expression and/or stimulation of other GPCRs²⁶. In the absence of modification of the total expression level nor coupling properties of 5-HT_{2B} when coexpressed with 5-HT_{1A}, we investigated putative changes in their expression at the plasma membrane. First, we evaluated 5-HT_{2B} density at the plasma membrane using again radioligand binding competition assays, this time on living, non-permeabilized, cells (See STAR Methods). Here, we observed that coexpression of the two receptors did not modify the 5-HT_{2B} K_i but significantly decreased its B_{max}, i.e. the amount of 5-HT_{2B} present at the plasma membrane. B_{max} for 5-HT_{2B} was indeed 60% lower when this receptor was expressed together with 5-HT_{1A} than when expressed alone (**Fig. 2A-B**). In contrast, 5-HT_{1A} plasma membrane expression levels were similar with and without coexpression of 5-HT_{2B} (not illustrated). To confirm these results, we performed biotinylation assay, and evaluated the ratio of the membrane/total protein expression level for each receptor (See STAR Methods). This showed that coexpression of the two receptors significantly decreased, by 31%, the amount of 5-HT_{2B} reaching the membrane (**Fig. 2C-D**), but did not impact 5-HT_{1A} membrane expression (**Fig. 2C-E**). Together, these data indicate that the 5-HT_{2B} membrane expression is reduced by coexpression of 5-HT_{1A}.

Neuronal co-distribution of 5-HT_{1A} and 5-HT_{2B} in somatodendritic compartment- Membrane proteins, including GPCRs, are targeted to specialized membrane domains, or clusters, via interactions with scaffolding proteins that are not only important for the regulation of synaptic transmission but also for the formation of signaling complexes. Receptor clustering controls signaling, trafficking, and cytoskeletal rearrangements around synapses²⁸. We previously showed that 5-HT_{2B} is localized in the somatodendritic compartment of transfected hippocampal cultured neurons and form clusters which reflect local accumulation of receptors²⁹. 5-HT_{2B} can positively regulate the activity of 5-HT neurons, in a manner opposite to 5-HT_{1A}²⁴. Independently, 5-HT_{1A} were shown to be expressed in the somatodendritic compartment of 5-HT and hippocampal neurons *in-vivo*^{30,31} and in cultures³². However, to date, the lack of selective and sensitive antibodies against these two receptors makes studies on endogenous receptors impossible. To assess their relative subcellular distribution, we thus transfected hippocampal neurons in cultures with plasmids encoding HA-tagged-5-HT_{2B} and myc-tagged-5-HT_{1A} (See STAR Methods). Both 5-HT_{1A} and 5-HT_{2B} located in the somatodendritic compartment, consistently with previous reports, but they displayed different distribution patterns: at the membrane of dendrites, 5-HT_{2B} were arranged in large clusters, whereas 5-HT_{1A} formed much smaller clusters, some of which are colocalized with 5-HT_{2B} clusters (**Fig. 3A**). We also observed, in these cultures of hippocampal neurons, that coexpression of 5-HT_{1A} decreased by 28% the membrane/total ratio of 5-HT_{2B} (**Fig. 3B**), confirming the effect previously observed in COS-7 cells (**Fig. 2**). Together, these data indicate that 5-HT_{2B} and 5-HT_{1A} are addressed to the somatodendritic compartment in neuron in culture, and may functionally interact.

Upon coexpression, selective stimulation of either 5-HT_{1A} or 5-HT_{2B} increases 5-HT_{2B} membrane clustering and maintains expression of 5-HT_{1A} at the plasma membrane- In transfected COS-7 cells and cultured hippocampal neurons, we observed that the addressing of 5-HT_{2B} to the plasma membrane was altered by coexpression of 5-HT_{1A}. Importantly, another parameter that can affect receptor function is its membrane clustering³³. Moreover, this distribution can be modified upon receptor stimulation, which will subsequently alter their function. We thus studied by confocal microscopy the distribution of 5-HT_{2B} and 5-

HT_{1A} expressed alone or together, at the plasma membrane of cultured hippocampal neurons, in basal condition and after stimulation of one receptor or the other. Selective agonists of each receptor were selected in order to limit possible cross-activation: the 5-HT_{1A} selective agonist 8-OHDPAT, which displays 1 nM affinity for 5-HT_{1A} and 5 μM affinity for 5-HT_{2B} and the preferential 5-HT_{2B} agonist BW723C86, which has 10 nM affinity for 5-HT_{2B}, over 1 μM for 5-HT_{1A}, and over 10-fold lower affinity for other 5-HT₂ receptors (see PDSP database <https://pdsp.unc.edu/databases/pdsp.php>). We first quantified the number and size of 5-HT_{2B} clusters and their integrated intensity, which reflects the density of receptors per cluster. We observed that when 5-HT_{2B} was expressed alone, its stimulation with the specific agonist BW (1 μM) for 20 min decreased the number of 5-HT_{2B} clusters (-51%) but increased their size (+97%) and intensity (+64%) (**Fig. 3C-D**). Interestingly, expression of 5-HT_{1A}, even in the absence of any stimulation, was sufficient to induce quite similar effects, i.e. to decrease the number of 5-HT_{2B} clusters (-36%) and to increase their area (+73%), but with no significant effect on their density (**Fig. 3C-D**). Selective stimulation by BW of the cotransfected neurons did not further significantly change these parameters.

Then, we quantified the plasma membrane expression level of 5-HT_{1A}. Selective stimulation of 5-HT_{1A} by 8-OH-DPAT (1 μM) led to a reduction of 5-HT_{1A} expression at the plasma membrane, as shown by the decrease in membrane 5-HT_{1A} fluorescence intensity over time (-41%), which suggests an internalization of the receptors (**Fig. 3E-F**). In contrast, coexpression of 5-HT_{2B} resulted in a +34% increase in 5-HT_{1A} expression at the plasma membrane, even in basal, non-stimulated condition, and prevented the decrease of membrane 5-HT_{1A} upon 8-OH-DPAT stimulation (**Fig. 3E-F**). Altogether, these results indicate that the coexpression of 5-HT_{2B} and 5-HT_{1A} increases the clustering (lower number, but bigger size of clusters) of 5-HT_{2B} and the membrane expression of 5-HT_{1A}, and prevents the effects of receptors agonists on their subcellular distribution, confirming a functional interaction between 5-HT_{2B} and 5-HT_{1A}.

Clusters of receptors are small objects, and the 200-nm diffraction limit of confocal microscopy does not allow isolation of nearby clusters (**Fig. 4A**). Using Stochastic Optical Reconstruction Microscopy (STORM) technique with a resolution up to 20 nm, we confirmed our initial observation (See STAR Methods): coexpression of 5-HT_{1A} with 5-HT_{2B}, with or without 5-HT_{2B} stimulation by BW, significantly decreased the number of 5-HT_{2B} cluster (-52% and -55%, respectively) and increased their area (+292% and +150%, respectively) (**Fig. 4B**). Thanks to its better resolution compared to confocal microscopy, this technique revealed in addition a significant potentiation by BW stimulation (2-fold) of the effects of 5-HT_{1A} coexpression on 5-HT_{2B} clustering (decrease in number and increase in area) (**Fig. 4B**). Together, these results confirmed that the coexpression of 5-HT_{1A} mimics some of the effects of 5-HT_{2B} stimulation by BW on its membrane distribution.

Selective stimulation of either 5-HT_{1A} or 5-HT_{2B} generates crossed effects on the other receptor's distribution at the plasma membrane - Since coexpression of both receptor was preventing most of the effect of the orthologous stimulation of either receptor, we asked whether stimulating one receptor would differentially impact the other receptor in cotransfected neurons. In coexpression condition, 5-HT_{1A} membrane expression was increased (+28%) compared to the single expression condition, as expected, but when we stimulated these cells with the selective 5-HT_{2B} agonist BW for 20 min, we reversed this increase and even induced a decrease (-28%) in 5-HT_{1A} membrane expression compared to the unstimulated condition (**Fig. 5A-B**). Conversely, in neurons expressing both 5-HT_{1A} and 5-HT_{2B}, and stimulated with the selective 5-HT_{1A} agonist 8-OH-DPAT for 20 min, we observed a decrease (-49%) in the number of 5-HT_{2B} cluster, together with an increase in their size (+99%) and intensity (+89%) (**Fig. 5C-F**). Thus, the stimulation of 5-HT_{1A} by its

agonist enhances the effects of 5-HT_{1A} coexpression on 5-HT_{2B} clustering (i.e. induction of less but bigger and brighter clusters) reported in **Fig. 3C-D**. These data suggest a cooperative association between 5-HT_{2B} and 5-HT_{1A} at the membrane of neurons, with 5-HT_{1A} stimulation increasing 5-HT_{2B} clustering and 5-HT_{2B} stimulation decreasing 5-HT_{1A} membrane expression.

Co-stimulation of both receptors by 5-HT suppresses 5-HT_{2B} effect on 5-HT_{1A} clustering- Since 5-HT_{1A} and 5-HT_{2B} respective agonists have different effects on the membrane clustering and localization of either receptor, we investigated the effect of co-stimulation with their natural ligand, 5-HT, on their distribution. Surprisingly, stimulation with 5-HT (1 μ M) did not modify 5-HT_{2B} cluster properties: neither the plasma membrane cluster density, nor the cluster size and intensity were affected by the coexpression of 5-HT_{1A} (**Fig. 6A**). On the contrary, stimulation with 5-HT decreased 5-HT_{1A} membrane expression by -39% compared to unstimulated condition (**Fig. 6B-C**), and close to what was observed after 8-OH-DPAT application (**Fig. 3E-F**). When coexpressed with 5-HT_{2B}, 5-HT_{1A} membrane expression increased by +24%, and 5-HT stimulation decreased this membrane expression by -50%, this effect being fully reversed by the selective 5-HT_{2B} antagonist, RS (**Fig. 6C**). This result supports the notion that stimulating both 5-HT_{2B} and 5-HT_{1A} by 5-HT reverses the 5-HT_{2B} ability to maintain the 5-HT_{1A} at the plasma membrane (**Fig. 6C**). These data indicate a differential crosstalk between 5-HT_{2B} and 5-HT_{1A} according to agonist selectivity, 5-HT vs. 8-OH-DPAT or BW.

Colocalized 5-HT_{2B}/5-HT_{1A} control the firing of 5-HT neurons by acting at apamin-sensitive SK channels- To study putative *in-vivo* colocalization of 5-HT_{2B} and 5-HT_{1A} in 5-HT neurons, we stereotactically injected in the B7 raphe nuclei of *Pet1-Cre⁺⁰* mice pAAV-EF1A-DIO-WPRE-pA viruses to specifically express Flag-tagged-5-HT_{1A} and HA-tagged-5-HT_{2B} together (**Fig. S2**) in DR 5-HT neurons as schematized on (**Fig. 7A**) (See STAR Methods). Confocal images of DR brainstem sections from these mice at low and intermediate magnification showed a fairly good colocalization of both receptors around cell bodies and proximal dendrites (**Fig. 7B**). Quantification analysis of confocal images of DR sections from these mice at high magnification revealed colocalization of both receptors in the somatodendritic compartment of 5-HT neurons (degree of overlap for 5-HT_{2B} over 5-HT_{1A} of 0.462 ± 0.053 and for 5-HT_{1A} over 5-HT_{2B} of 0.465 ± 0.087) (**Fig. 7C**) (See STAR Methods).

The serotonergic tone of the DR neurons is known to be negatively regulated by 5-HT_{1A} and activation of 5-HT_{2B} by BW can increase 5-HT neurons firing activity²⁴. To investigate putative contribution of these receptor interactions on the firing of 5-HT neurons, we performed patch-clamp recording on identified 5-HT neurons of acute brainstem slices from either control mice or mice selectively lacking 5-HT_{2B} expression in 5-HT neurons. For this purpose, we used as control GFP^{5-HT} mice and 2B-KO^{5-HT}::GFP^{5-HT} mice, both of which expressing GFP exclusively by 5-HT neurons, and studied action potential frequency in response to depolarizing current steps (See STAR Methods). Basal Frequency-Intensity (F-I) curves did not differ between GFP^{5-HT} and 2B-KO^{5-HT}::GFP^{5-HT} 5-HT neurons (**Fig. 7D**), nor the resting membrane potential and input resistance (**Fig. 7E**). In the presence of the 5-HT_{1A} agonist 8-OH-DPAT (30 nM), the firing frequency of GFP^{5-HT} 5-HT neurons was decreased; the firing frequency of 2B-KO^{5-HT}::GFP^{5-HT} 5-HT neurons became significantly higher than that of GFP^{5-HT} 5-HT neurons (**Fig. 7F**), or of unstimulated 2B-KO^{5-HT}::GFP^{5-HT} 5-HT neurons (not illustrated); the resting membrane potential and input resistance remained similar (**Fig. 7G**), but different from unstimulated neurons, with a reduction in resting potential (-65 mV vs. -77 mV) and in input resistance (771 MOhm vs. 350 MOhm) (**Fig. S1**).

SK channels are responsible for mAHPs, that control the tonic firing of DR 5-HT neurons. When a selective SK2/3 channel blocker, Apamin (20 nM) was applied together with 8-OH-DPAT (30 nM), F-I curves for GFP^{5-HT} and 2B-KO^{5-HT}::GFP^{5-HT} 5-HT neurons became again similar (**Fig. 7H**) and higher than the unstimulated condition, with resting membrane potential and input resistance remaining similar and close to the value obtained after 8-OHDPAT stimulation (**Fig. 7I**). These results indicate that, in the absence of 5-HT_{2B} (i.e. in brainstem slices from 2B-KO^{5-HT}::GFP^{5-HT} mice), 5-HT neuron firing activity is increased upon 5-HT_{1A} stimulation by 8-OH-DPAT, when 5-HT_{1A} can be internalized. In the presence of 5-HT_{2B} (i.e. in GFP^{5-HT} mice), 5-HT neuron firing activity is decreased when 8-OH-DPAT cannot trigger internalization of 5-HT_{1A}, supporting a link between receptor functions and trafficking.

DISCUSSION

Combined with our previous investigations about 5-HT_{2B} functions in 5-HT neurons²⁴ and extensive studies on 5-HT_{1A} activity as autoreceptors of these neurons, the present work demonstrates that 5-HT_{1A}/5-HT_{2B} interactions are implicated in the regulation of serotonergic tone, which is a prime importance for mood disorders. We found that 5-HT_{1A} and 5-HT_{2B} are colocalized upon overexpression in hippocampal cultures and in 5-HT neurons *in-vivo*, and can interact together to form dimers. Coexpression of these two receptors impacts on their membrane expression level and/or concentration in clusters, which can be further regulated by stimulation with various agonists.

Different techniques allowed us to validate the reciprocal effects of 5-HT_{1A} and 5-HT_{2B} on their subcellular distribution. Confocal microscopy was used to analyze and compare, in various conditions, the number of clusters, their size and the density of receptors per cluster. With a resolution up to ~20 nm, STORM allows an accurate analysis of receptor spatial distribution and confirmed that 5-HT_{2B} are locally concentrated in clusters at the membrane of hippocampal neurons. Moreover, this technique confirmed that stimulation of 5-HT_{2B} by its selective agonist, BW, triggers its aggregation into larger and denser clusters (summarized in **Fig. 8A**). 5-HT_{1A} coexpression also increases 5-HT_{2B} clustering, as assessed by the significant decrease in the number but increase in the area of 5-HT_{2B} clusters, and 5-HT_{2B} aggregation is further enhanced upon selective stimulation of either 5-HT_{2B} (by BW as evidenced by STORM) or 5-HT_{1A} (by 8-OH-DPAT) (**Fig. 8B**). On the other hand, stimulation of 5-HT_{1A} by its selective agonist 8-OH-DPAT decreases its membrane expression if they are expressed alone (**Fig. 8A**), but this down-regulating effect of 8-OH-DPAT on 5-HT_{1A} is not observed when 5-HT_{2B} is coexpressed (**Fig. 8B**). It has been shown that 5-HT_{1A} autoreceptors desensitize and are internalized upon stimulation³⁴ and especially after chronic exposure to high extracellular concentration of 5-HT, a condition induced for example by chronic SSRI treatment¹⁸.

The mechanisms of 5-HT_{1A} internalization involve phosphorylation by PKA and PKC since phosphorylation sites were identified in 5-HT_{1A}³⁵. Stimulation by 8-OH-DPAT of 5-HT_{1A} recruits β -arrestin2⁵, which, with GRK2, triggers its internalization via clathrin-coated pits³⁶, and signaling to ERK1/2³⁷. Concerning 5-HT_{2B}, we showed that 5-HT_{2B} internalization was dependent on β -arrestin-2, GRK2,3 and clathrin when stimulated either by 5-HT or BW, although stimulation by BW internalized 5-HT_{2B} more than twice faster than 5-HT³⁸. Here, we show that internalization of 5-HT_{1A} by 8-OH-DPAT is prevented by the presence of 5-HT_{2B}. 5-HT_{1A} internalization is observed only when 5-HT_{2B} is stimulated by BW or by 5-HT and 5-HT_{2B} internalization is insensitive to the presence of 5-HT_{1A}. This finding supports a competition between 5-HT_{1A} and 5-HT_{2B} for desensitization machinery: 5-HT_{1A} internalization being prevented unless 5-HT_{2B} are stimulated. Of note, PKC, which can be activated by 5-HT_{2B}, was shown to induce a rapid phosphorylation of 5-HT_{1A}³⁵. Nevertheless, the precise mechanisms underlying internalization and desensitization of 5-HT_{1A} and 5-HT_{2B} in 5-HT neurons remain to be identified.

Oligomerization of GPCRs is a well-documented process that can be essential for their trafficking to the plasma membrane, agonist binding, and signaling^{39,40}. Metabotropic 5-HT are able to form homo or heterodimers with each other or with non-5-HT receptors²⁶, which can impact on their function. For example, 5-HT_{1A}/5-HT₇ heterodimerization decreases G α i and subsequent GIRK activation downstream of 5-HT_{1A} stimulation, without affecting 5-HT₇ signaling pathway³². 5-HT_{1A} and 5-HT_{2A} (close relative to 5-HT_{2B}) can form oligomers⁴¹ in pyramidal neurons of the prefrontal cortex. Coexpression of these two receptors triggers 5-HT_{1A}-dependent inhibitory responses, 5-HT_{2A}-dependent excitatory responses, and biphasic responses in which excitation follows a brief inhibition likely depending on respective expression levels of these receptors^{42,43}. In cells coexpressing 5-

HT_{1B} (close relative to 5-HT_{1A}) and 5-HT_{2B}, and in the absence of direct interaction, stimulation by 5-HT makes 5-HT_{2B} to internalize via its classic clathrin pathways but also via 5-HT_{1B}-triggered GRK2,3 activation and Caveolin1-dependent pathways³⁸. Here, we show that coexpression of 5-HT_{1A} and 5-HT_{2B}, despite no apparent impact on their classical second messenger signaling, has an effect on the expression level of both receptors at the plasma membrane (**Fig. 8B**). The specific interacting sequence in the heteromer between the 5-HT_{2B} and the 5-HT_{1A} remains to be identified.

Coexpression of 5-HT_{1A} with 5-HT_{2B} favors the clustering of 5-HT_{2B}, mimicking the effect of 5-HT_{2B} stimulation, and this is further enhanced by selective stimulation of 5-HT_{1A} with 8-OH-DPAT. We can thus conclude that 5-HT_{1A}, without or with stimulation, can control 5-HT_{2B} membrane clustering. Reciprocally, while homologous 5-HT_{1A} agonist stimulation by 8-OH-DPAT decreases 5-HT_{1A} membrane expression if this receptor is expressed alone, the coexpression with 5-HT_{2B} increases 5-HT_{1A} membrane level and maintains it at the neuronal membrane, counteracting the effect of 5-HT_{1A} stimulation by its own agonist 8-OH-DPAT (**Fig. 8B**). Therefore, the dynamic regulation of 5-HT_{1A} membrane expression not only depends on the ligand but also on the panel of receptors expressed by the neuron. In addition, we show that 5-HT, the physiological ligand of 5-HT_{1A} and 5-HT_{2B}, has no significant impact on the distribution of 5-HT_{2B} coexpressed with 5-HT_{1A}. Interestingly, we found that 5-HT stimulation abolishes 5-HT_{2B} positive effect on 5-HT_{1A} membrane expression, and decreases 5-HT_{1A} membrane expression level. This decrease in 5-HT_{1A} membrane expression is entirely 5-HT_{2B}-dependent since it can be restored by applying the highly selective 5-HT_{2B} antagonist RS, confirming the observation that BW reduces 5-HT_{1A} membrane expression only in the presence of 5-HT_{2B}. Together, our results demonstrate that modulation of 5-HT_{1A} membrane expression can be triggered not only by its own stimulation, but also through 5-HT_{2B} activation, confirming their functional crosstalk.

We previously reported that *in-vivo* injection of BW attenuated 8-OH-DPAT-induced hypothermia and inhibition of 5-HT neurons firing. These two effects of 8-OH-DPAT are attributed to the activation of 5-HT_{1A} expressed by 5-HT neurons. These data suggested that 5-HT_{2B} counteracted 5-HT_{1A} negative effects on 5-HT neurons²⁴. These 5-HT_{2B} positive effects were also substantiated by cell-attached electrophysiological recording showing that 5-HT_{2B} activation by BW increased 5-HT neurons firing activity²⁴. Here, using current-clamp recording in *ex-vivo* identified 5-HT neurons, we observed that the increase in firing frequency of action potentials upon raising current steps was similar in GFP^{5-HT} mice and in 2B-KO^{5-HT::GFP^{5-HT}} mice. Stimulation by 8-OH-DPAT decreased the firing frequency of 5-HT neurons from GFP^{5-HT} mice, i.e. in the presence of 5-HT_{2B} and 5-HT_{1A}. The coexpression of 5-HT_{1A} with 5-HT_{2B} increases 5-HT_{1A} membrane expression, and blocks its internalization upon 8-OH-DPAT stimulation (**Fig. 8C**), supporting that 5-HT_{2B} is important to stabilize 5-HT_{1A} at the plasma membrane, and to limit its agonist-induced internalization. This coexpression likely favors 5-HT_{1A}-dependent activation of GIRK channels. The basal GIRK conductance contributes the intrinsic membrane properties of DR neurons and, in particular, the GIRK2 subunit contributes to set the resting membrane potential and input resistance of DR neurons⁴⁴. It is therefore, not surprising to find that 8-OHDPAT triggered a reduction in resting potential and in input resistance (**Fig. S1**), which were not further affected by apamin since stimulation of 5-HT_{1A} is known to activate GIRK channels¹¹. By contrast, stimulation by 8-OH-DPAT in the presence of apamin significantly increased the firing frequency of 5-HT neurons from GFP^{5-HT} mice compared to unstimulated neurons, and similar to that of 2B-KO^{5-HT::GFP^{5-HT}} neurons i.e. in the absence of 5-HT_{2B}. This finding supports that in the absence of 5-HT_{2B}, 8-OH-DPAT triggers internalization of 5-HT_{1A} and favors its coupling to SK inhibition (**Fig. 8C**) as previously reported¹⁶; in the presence of 5-HT_{2B}, 8-OH-DPAT reduces the ability of 5-HT_{1A} to couple to SK channel inhibition. The observation that

coexpression with 5-HT_{1A} increases the size of 5-HT_{2B} clusters that is potentiated by 8-OH-DPAT, may finally support the 5-HT_{2B} ability to couple to SK channel inhibition in this condition, likely by competition with 5-HT_{1A}.

Using current-clamp recordings, we previously showed that overexpression of 5-HT_{2B} in 5-HT neuron triggered a significant increase in the basal (non-stimulated) firing frequency compared to controls²⁴. Apamin was shown to increase the burst firing of DR 5-HT neurons leading to increased 5-HT release¹⁴ in a similar way as the SSRI fluoxetine⁴⁵ or as the 5-HT_{2B} agonist BW^{21,24}. Furthermore, mice exposed to chronic social isolation develop depressive-like state that can be reversed by SSRIs only in the presence of 5-HT_{2B}⁴⁶, or by apamin, which regulates 5-HT firing pattern⁴⁷. Together, these data support that interaction between 5-HT_{2B}/5-HT_{1A} and their stoichiometry are required to control proper firing of 5-HT neurons by regulating mAHP that condition SSRIs efficacy.

LIMITATIONS OF THE STUDY

In this work, intracellular interactions between 5-HT_{1A} and 5-HT_{2B} data are mainly based on overexpression studies either on transfected cells and hippocampal neurons or on *in-vivo* infected 5-HT neurons. When reliable antibodies will be available, it will be necessary to further validate these findings on endogenous receptors *in-vivo*. Although established on *ex-vivo* endogenously expressed receptors, it remains to be determined *in-vivo* if 5-HT_{2B} stimulation controls directly (e.g. by PKC activation and thus by phosphorylation) SK channels, and/or 5-HT_{1A} or if this regulation is relying exclusively on 5-HT_{1A}/5-HT_{2B} dimeric interactions and/or competition to common effectors.

STAR Methods

Resources availability

Lead contact

Further information and requests for resources should be directed to and will be fulfilled by the lead contact, Luc Maroteaux (luc.maroteaux@upmc.fr).

Materials availability

All newly created materials can be accessed by asking the authors.

This study did not generate new unique reagents.

Data and Code Availability

N/A

Any additional information

None

Experimental Model And Subject Details

Animals

Floxed mice, $Htr2b^{tm2Lum}/Htr2b^{tm2Lum}$, (IMSR Cat# EM:05939, RRID: IMSR_EM:05939) ($Htr2b^{lox/lox}$, WT) were generated on a mixed B6;129S2 background and backcrossed >10 times onto the 129S2 strain. $Htr2b^{lox/lox}$ mice were inactivated for $Htr2b$ in 5-HT neurons by crossing with $129S2.Cg-Tg(Fev-cre)^{1Esd}/0$ (IMSR Cat# JAX:012712, RRID:IMSR_JAX:012712) (ePet1-Cre BAC transgenic mice or $Pet1-Cre^{+/0}$)⁴⁸ generating $129S2.Cg-Pet1-Cre^{+/0}; Htr2b^{lox}/Htr2b^{lox}$ conditional knockout mice (2B-KO^{5-HT}) and littermate controls (WT)²⁴.

For electrophysiology, these strains of mice were further crossed with $Gt(ROSA)26Sor^{m1(CAG-EGFP)^{Fsh}}/Gt(ROSA)26Sor^{+}$ (MGI Cat# 4420760, RRID:MGI:4420760) (Rosa26;CAG-loxP-STOP-loxP-EGFP or RCE) that after crossing with $Pet1-Cre^{+/0}$ generated (GFP^{5-HT}) that express GFP in Pet1-positive 5-HT neurons only after Cre recombination, and in the presence of floxed allele generated conditional knockout mice (2B-KO^{5-HT}::GFP^{5-HT}) that express GFP but no 5-HT_{2B} in Pet1-positive 5-HT neurons. Males and females mice were used at 25-31 postnatal days.

All mice were bred at our animal facility. Food and water were available *ad libitum*. The temperature was maintained at 21±1°C, under 12/12h light/dark. Mice were moved to the experimental room in their home cage at least 5 days prior to testing to allow for habituation to the environment.

Sprague-Dawley rat pups used for primary cultures of hippocampal neurons were taken at embryonic day 19 from Janvier labs.

Ethical statement

All experiments involving mice were approved by the local ethical committee, Ethical Committee for Animal Experiments of the Sorbonne University, Charles Darwin C2EA - 05 (authorizations N°APAFIS#28228, and AFAFIS#28229). All efforts were made to minimize animal suffering.

Methods Details

Results are described in accordance with the ARRIVE guidelines for reports in animal research⁴⁹ as detailed in Table S2. Numbers of animals for each test are reported in the figure legends.

Viral constructs and stereotaxic injection

To express HA-tagged 5-HT_{2B} and Flag-tagged 5-HT_{1A} specifically in 5-HT neurons, we use a Double floxed Inverse Orientation (DIO) adeno-associated virus (AAV) construct that allows Cre-mediated expression of the transgene (pAAV-EF1A-DIO-WPRE-pA vector; RRID Addgene_39320)²⁴ (**Fig. S2**). The viruses packaged into AAV2.9 serotype with titers of 10¹²-10¹³ viral particles / ml were obtained (UNC Vector Core, Chapel Hill USA). Both AAVs were stereotaxically injected in the B7 raphe nuclei of males or females *Pet1-Cre*⁺⁰ mice at 6 weeks of age⁵⁰. They were used 3 weeks after surgery for histological procedures. Respective expression was assessed by immunostaining using a mouse anti-HA antibody (1:500; Cell Signaling#2367, RRID AB_10691311 and a rabbit anti-Flag (1:500; Cell Signaling#14793 RRID AB_2572291 followed by Cy5-conjugated donkey anti-mouse (1.9 µg/ml; Jackson ImmunoResearch#715-175-150, RRID AB_2340819) and the Cy3-conjugated goat anti-rabbit antibody (1.9 µg/ml; Jackson ImmunoResearch#111-165-003, RRID AB_2338000).

Culture of COS-7 cells

COS-7 cells were cultured as monolayers in Dulbecco's modified Eagle's medium (DMEM) (Gibco, Invitrogen) supplemented with 10% fetal calf serum (Biowest) and 1% penicillin/streptomycin (Sigma), in 9-cm dishes (Falcon). Cells were incubated at 37 °C in a 5% CO₂ atmosphere. Cells 70% confluent in 6-well plates were used for inositol phosphate accumulation and biotinylation experiments, in 24-well plates for membrane binding, in 9-cm dishes for total binding and co-immunoprecipitation/Western-blot and in 96-well plates for BRET experiments. They were transfected with pCAGG vectors using the Genejuice transfection reagent (Merck Millipore) in complete DMEM, according to the manufacturer's instructions. Twenty-four hours before the experimental test, cells were incubated in a serum-free medium.

Co-immunoprecipitation

Co-immunoprecipitation and Western-blotting were performed in COS-7 cells transfected with a total of 10 µg of DNA per 9-cm dishes with a ratio of 7:3 (HA-5-HT_{2B} / empty vector; empty vector / myc-5-HT_{1A}; HA-5-HT_{2B} / myc-5-HT_{1A}) and maintained in culture for three days before harvesting²⁷. Cells were centrifuged and suspended in CHAPS lysis buffer (50 mM Tris-HCl, pH 7.4, 0.05 mM EDTA, 10 mM CHAPS, and protease inhibitor cocktail, pH 7.4) and sonicated three times for 30 s. Cells were next solubilized for 5 h at 4°C under gentle agitation. Lysates were centrifuged (20,000 x g) in order to pellet non-solubilized membranes. Protein concentrations in supernatant were measured using the Pierce™ Coomassie Protein Assay Kit. Lysates were co-immunoprecipitated with anti-HA beads (HA-Tag C29F4 Rabbit mAb Sepharose® Bead Conjugate Cell Signaling #3956 RRID:AB_10695091) overnight at 4 °C under gentle agitation. Total lysate and immunoprecipitated proteins were separated by SDS/PAGE onto 10% polyacrylamide gels and transferred electrophoretically to nitrocellulose membranes. Inputs represent 5% of the total protein amount used for immunoprecipitations. Blots were probed with rabbit anti-HA (1:1,000; Cell Signaling#3724, RRID AB_1549585) or mouse anti-myc (1:1,000; Cell Signaling#2276, RRID AB_331783). Antibodies (1:10,000; goat anti-mouse-IR800, Advansta# R-05060-250 and goat anti-rabbit-IR700, Advansta# R-05054-250) were used as secondary antibodies. Immunoreactive bands were detected using the Odyssey software. At least three independent experiments were performed.

Bioluminescence resonance energy transfer (BRET)

BRET assays were performed in 6-well plates. COS-7 cells were transfected with 30-100 ng of plasmid DNA coding for the BRET donor (5-HT_{2B}luc)²⁷ and an increasing amount of BRET acceptor plasmids (5-HT_{1A}-YFP; from 100 to 4000 ng/well). Twenty-four hours later, the cells were trypsinized (trypsin 0.05% EDTA; Invitrogen) and plated in 96-well plates (50,000 cells/well). The day after, the luciferase substrate, coelenterazine-h, was added in each well at a 5 μ M final concentration. Using a Mithras LB940 plate reader, luminescence and fluorescence were then measured simultaneously at 485 and 530 nm, respectively. The BRET ratios were calculated as ((emission at 530 nm/emission at 485 nm)-(background at 530 nm/background at 485 nm)) and were plotted as a function of ((YFP-YFP0)/YFP0)/(Rluc/Rluc0). The background corresponds to signals in cells expressing the Rluc fusion protein alone under the same experimental conditions. YFP is the fluorescence signal at 530 nm after excitation at 485 nm, and Rluc is the signal at 485 nm after addition of coelenterazine-h. YFP0 and Rluc0 correspond to the values in cells expressing the Rluc fusion protein alone.

Binding experiments

Membrane radioligand binding assay

Membrane binding assays were performed on transfected cells plated in 9-cm dishes²⁴. Cells were first washed with PBS, scraped into 10 ml of PBS on ice, and then centrifuged for 5 min at 1,000 g. Cell pellets were dissociated and lysed in 2 ml of binding buffer (50 mM Tris-HCl, 10 mM MgCl₂, 0.1 mM EDTA, pH 7.4) and centrifuged for 30 min at 10,000 g. Membrane preparations were then resuspended in binding buffer to obtain a final concentration of 0.2–0.4 mg of protein/well. Aliquots of membrane suspension (200 μ l/well) were incubated with 25 μ l/well of ³H-mesulergine or ³H-8-OH-DPAT at a final concentration between 1/2 to 1/10 Kd for each 5-HT receptor, diluted in binding buffer and 25 μ l/well of increasing concentrations of heterologous compound. 5-HT_{2B} agonist BW-723C86 (BW) or antagonist RS-127445 (RS), 5-HT_{1A} agonist 8-OH-DPAT or antagonist NAN-190 (NAN) were from Tocris (UK). Competition was performed at concentration between 10⁻¹¹ to 10⁻⁵ M, diluted in binding buffer in 96-well plates for 60 min at room temperature. Membranes were harvested by rapid filtration onto Whatman GF/B glass fiber filters (Brandell) pre-soaked with cold saline solution and washed three times. Filters were placed in 6-ml scintillation vials and counted. Data in disintegrations/min were converted to femtomoles and normalized to protein content (ranging from 0.1 to 1 mg/well). At least three independent experiments were performed in duplicate.

Non-permeabilized whole cell radioligand binding assay

Cells expressing 5-HT_{2B} and/or 5-HT_{1A} were plated in 24-well plates. Twenty-four hours before the experiment, the cells were incubated in serum-free medium overnight. The next day, the medium was replaced by 400 μ l/well of Krebs-Ringer/Hepes buffer (130 mM NaCl, 1.3 mM KCl, 2.2 mM CaCl₂, 1.2 mM NaH₂PO₄, 1.2 mM MgSO₄, 10 mM Hepes, 10 mM glucose, pH 7.4). Then, 50 μ l of [³H]-mesulergine were diluted in Krebs-Ringer/Hepes buffer at a final concentration 1/2 Kd value of 5-HT_{2B}. The radioligand was competed with 50 μ l of increasing concentrations of non-radioactive BW, also diluted in Krebs-Ringer/Hepes buffer. Cells were then incubated for 30 min at room temperature and then washed twice on ice with cold PBS. Washed cells were solubilized by the addition of 500 μ l of SDS 1%. The next day, 3 ml of scintillation mixture were added to the samples, and the radioactivity was counted. Data in disintegrations/min were converted to femtomoles and normalized to protein content (0.2–0.4 mg of protein/well). At least three independent experiments were performed in duplicate.

Second messenger measurements

COS-7 cells were transfected with 3 µg of DNA (1:1 ratio for co-transfection) in 6-well plates using Genejuice transfecting reagent in complete medium. Twenty-four hours later the cells were trypsinized (trypsin 0.05% EDTA; Invitrogen) and plated in 96-well plates (30,000 cells/well). The next day, the complete medium was replaced by a serum-free medium.

HTRF IP accumulation

The day of the experiment, media were replaced by stimulation buffer with LiCl to prevent IP1 degradation (NaCl, 146 mM, KCl, 4.2 mM, MgCl₂, 0.5 mM, CaCl₂, 1 mM, Hepes, 10 mM, glucose, 5.5 mM, LiCl, 50 mM, pH7.4). Cells were stimulated during 2 h at 37°C with different concentrations of BW (10⁻¹¹ to 10⁻⁶ M in stimulation buffer). Stimulation solution was replaced by a lysis buffer (IP one HTRF Kit, Cisbio, France) during 1 h. Lysates were distributed to 384-well plates, and IP was labeled using HTRF reagents. The assay is based on a competitive format involving a specific antibody labeled with terbium cryptate (donor) and IP coupled to d2 (acceptor). After a 1-h incubation with HTRF reagent, the plate was read using Mithras LB940 plate reader according to the manufacturer's instructions. Modelization and EC50 calculation were done using GraphPad Prism 7 software. At least three independent experiments were performed in duplicate.

Surface biotinylation

Surface biotinylation was performed on transfected COS-7 cells. Briefly, cells were initially washed twice in cold PBS and subsequently incubated in PBS containing 1 mg/ml Sulfo-NHS-SS-Biotin for 30 min at 4°C to allow for labelling of all surface membrane proteins. Reaction was stopped by applying a quench solution (100 mM Tris pH 8 in PBS) to remove excess biotin. Biotinylated cells were then homogenized in RIPA buffer containing 25 mM Tris (pH 7.6), 150 mM NaCl, 1% TritonTM X-100, 0.5% sodium deoxycholate, 0.1% SDS, 1mM NaF and a cocktail of protease inhibitors (Roche). The lysate was centrifuged at 21,000 g to remove nuclei and cellular debris. A small amount of the lysate was removed and constituted the "input" or total lysate. Then, 100 µl of StreptAvidin beads (Thermo Scientific Inc) were added to 40 µg of protein lysate and placed on a rotator at 4°C overnight. Samples were then washed three times in RIPA buffer and a fourth times in RIPA buffer without detergents (25 mM Tris pH 7.6, 150 mM NaCl, 0.5% TritonTM X-100; protease inhibitor); beads were pulled-down after each wash by 1 min centrifugation. Bound proteins were eluted in SDS reducing buffer and heated at 70°C for 5 min.

Western blotting

For co-immunoprecipitation and surface biotinylation experiments, total lysate and immunoprecipitated proteins were separated by SDS/PAGE onto 10% acrylamide gels and transferred electrophoretically to nitrocellulose membranes. Blots were probed with rabbit anti-HA (1:1,000; Cell Signaling#3724, RRID AB_1549585) or mouse anti-myc (1:1,000; Cell Signaling#2276, RRID AB_331783). Secondary antibodies (1:10,000; goat anti-mouse-IR800, Advansta# R-05060-250 and goat anti-rabbit-IR700, Advansta# R-05054-250) were used as secondary antibodies. Immunoreactive bands were detected using the Odyssey software. At least three independent experiments were performed.

Hippocampal neuronal culture and transfection.

Hippocampal neurons were prepared from embryonic day 19 Sprague-Dawley rat pups²⁹. Dissected tissues were trypsinized (0.25% v/v) and mechanically dissociated in HBSS (CaCl₂ 1.2 mM, MgCl₂ 0.5 mM, MgSO₄ 0.4 mM, KCl 5 mM, KH₂PO₄ 0.44 mM, NaHCO₃ 4.1 mM, NaCl 138 mM, Na₂HPO₄ 0.34 mM, D-Glucose 5.5 mM) containing 10 mM Hepes (Invitrogen). Dissociated cells were plated on glass coverslips (Assistent) precoated with 55 µg/ml poly-D,L-ornithine (Sigma-Aldrich) in plating

medium composed of MEM supplemented with horse serum (10% v/v; Invitrogen), L-glutamine (2 mM), and Na pyruvate (1 mM, Invitrogen) at a density of 3.4×10^4 cells/cm² and maintained in humidified atmosphere containing 5% CO₂ at 37°C. After attachment for 2-3 h, cells were incubated in maintenance medium that consists of Neurobasal medium supplemented with B27, L-glutamine (2 mM), and antibiotics (Invitrogen). Each week, one-third of the culture medium volume was renewed. Neuronal transfection with plasmids encoding HA-5-HT_{2B}, Myc-5-HT_{1A} and eGFP were performed at 13–14 DIV using Transfectin (Bio-Rad), according to the instructions of the manufacturer (DNA/lipofectant ratio of 1:3), with 1.5 µg of plasmid DNA per 20-mm well. The following ratio of plasmid DNA was used in co-transfection experiments: 1:0.3:0.2 µg for HA-5-HT_{2B} / Myc-5-HT_{1A} / eGFP. Experiments were performed 7–10 days after transfection.

Immunostaining

The total (membrane plus intracellular) pools of HA-5-HT_{2B} and myc-5-HT_{1A} were revealed with immunocytochemistry in fixed and permeabilized cells, whereas the membrane pool was done in non-permeabilized cells. To label the total pool of receptors, cells were fixed for 10 min at room temperature in paraformaldehyde (PFA; 4% w/v; Sigma) and sucrose (20% w/v; Sigma) solution in PBS. Cells were then washed in PBS, and permeabilized for 4 min with Triton X-100 (0.25% v/v) in PBS. After these washes, non-specific staining was blocked for 30 min with goat serum (20% v/v; Invitrogen) in PBS. Neurons were then incubated for 1 h with either rabbit anti-HA antibodies (1:500; Cell Signaling #3724, RRID AB_1549585) or mouse anti-myc antibodies (1:500; Cell Signaling #2276, RRID AB_331783) in PBS supplemented with Goat Serum (GS) (3% v/v). Cells were then washed three times and incubated for 45 min with Cy5-conjugated donkey anti-mouse or Alexa 488 donkey anti-mouse antibodies (1.9 µg/ml; Jackson ImmunoResearch # 715-175-150, RRID AB_2340819 or #715-175-150, RRID AB_2336933) or the Cy3-conjugated goat anti-rabbit antibodies (1.9 µg/ml; Jackson ImmunoResearch # 111-165-003, RRID AB_2338000) in PBS-goat serum blocking solution, washed, and mounted on slides with Mowiol 4-88 (48 mg/ml). In experiments using BW723C86, 5-HT, or 8-OH-DPAT, drugs were diluted in imaging medium and applied to neurons for 10 or 20 min at 1 µM final concentration before fixation and immunolabeling. The imaging medium consisted of phenol red-free MEM supplemented with glucose (33 mM), Hepes (20 mM), glutamine (2 mM), Na⁺-pyruvate (1 mM), and B27 (1X, Invitrogen). Sets of neurons to be compared were labeled and imaged simultaneously.

Fluorescence image acquisition and cluster analyses

Fluorescence image acquisition and analyses were performed on images obtained with a Leica SP5 confocal microscope using the LAS-AF program (Leica)²⁹. Stacks of 16–35 images were acquired using a 100 X objective with an interval of 0.2 µm and an optical zoom of 1.5. Image exposure time was determined on bright cells to avoid pixel saturation. All images from a given culture were then acquired with the same exposure time. Quantifications of clusters were performed using MetaMorph software (Roper Scientific) on projections (sum of intensity) of confocal optical sections. For each cell, a region of interest (ROI) was chosen.

For 5-HT_{2B} cluster analysis, images were first flattened background filtered (kernel size, 3 x 3 x 2) to enhance cluster outlines, and a user-defined intensity threshold was applied to select clusters and avoid their coalescence. Thresholded clusters were binarized, and binarized regions were outlined and transferred onto raw data to determine the mean 5-HT_{2B} cluster number, area and fluorescence intensity. For quantification, clusters comprising at least 3 pixels were considered. The dendritic surface area of regions of interest was measured to determine the number of clusters per 10 µm². Due to the variability between cultures, the number of clusters in each culture was normalized to the respective control values, allowing for comparisons between cultures.

As the 5-HT_{1A} presents an expression pattern in small clusters, the average fluorescent intensity per pixel was measured in a defined ROI. For each culture, we analyzed 7-12 dendrites per experimental condition. A total of about 10 neurons were analyzed per condition from three to five independent cultures. The experimenter was blind to the culture treatment.

Quantitative colocalization analysis.

Two-channel confocal microscopic images were analyzed for colocalization with the Manders' colocalization coefficient, using the JACoP plug-in⁵¹ for ImageJ (National Institute of Health, Bethesda, MD). In order to facilitate analysis, 100 × 100 μm areas were arbitrarily selected close to the midline DR. This analysis was performed on three independent viral co-infections. Similar results were obtained in each independent experiment. Image stacks were converted to binary images with the threshold function of the JACoP plug-in and manually adjusted. The Manders' coefficient determines the degree (from 0 to 1) of overlap between red (5-HT_{2B}) and green (5-HT_{1A}) channels⁵².

STORM imaging

STochastic Optical Reconstruction Microscopy (STORM) imaging was conducted on an inverted N-STORM Nikon Eclipse Ti microscope equipped with a 100× oil-immersion TIRF objective (NA 1.49) and an Andor iXon Ultra 897 EMCCD camera using 405 and 638 nm lasers from Coherent. Movies of 30,000 frames were acquired at frame rates of 50 Hz. The z position was maintained during acquisition by a Nikon Perfect Focus System and multicolor fluorescent microspheres (Tetraspeck, Invitrogen) were used as markers to register long-term acquisitions and correct for lateral drifts. Single-molecule localization and 2D image reconstruction was conducted as described in⁵³ by fitting the point-spread function of spatially separated fluorophores to a 2D Gaussian distribution. The surface of clusters and the densities of molecules per μm² were measured in reconstructed 2D images through cluster segmentation based on detection densities. The threshold to define the border was set to 1000 detections/μm². All pixels containing <2 detections were considered empty, and their intensity value was set to 0. The intensity of pixels with 2 detections was set to 1. The resulting binary image was analyzed with the function "regionprops" of Matlab to extract the surface area of each cluster identified by this function. Density was calculated as the total number of detections in the pixels belonging to a given cluster, divided by the area of the cluster.

Electrophysiology

For patch clamp experiments, 260 μm-thick brain coronal slices were prepared from GFP^{5-HT} mice (control) and 2B-KO^{5-HT::GFP^{5-HT}} mice at 4 weeks (25-31 postnatal days) that express GFP only in Pet1-positive 5-HT neurons. The brain extraction and slicing was performed in ice-cold (0–4°C) oxygenated (95% O₂-5% CO₂) solution containing 110 mM choline chloride, 2.5 mM KCl, 25 mM glucose, 25 mM NaHCO₃, 1.25 mM NaH₂PO₄, 0.5 mM CaCl₂, 7 mM MgCl₂, 11.6 mM L-ascorbic acid, and 3.1 mM sodium pyruvate. Slices were then stored in artificial cerebro-spinal fluid (aCSF) containing 125 mM NaCl, 2.5 mM KCl, 25 mM glucose, 25 mM NaHCO₃, 1.25 mM NaH₂PO₄, 2 mM CaCl₂, and 1 mM MgCl₂ (pH 7.2, maintained by continuous bubbling with 95% O₂-5% CO₂). Slices were incubated in aCSF at 32°C for 20 min and then at room temperature (20–25°C). Slices were transferred to the recording chamber where they were continuously superfused with oxygenated aCSF (30–32°C). To block synaptic transmission, we added to the aCSF 6-cyano-7-nitroquinoxaline-2,3-dione (CNQX; 10 μM, Hello Bio), D-2-amino-5-phosphonopentanoic acid (D-APV; 50 μM, Hello Bio) and SR95531 hydrobromide (GABA_Azine, 10 μM, Hello Bio). We also used (±) 8-hydroxy-2-(di-n-propylamino)tetralin hydrobromide (8-OH-DPAT; 30nM, SIGMA) and Apamin (20nM, Hello Bio) to activate 5-HT_{1A} and block SK channels, respectively. Current clamp and voltage clamp recordings were performed with pipettes (5- to 7-MΩ resistance) prepared from borosilicate glass (BF150-86-10; Harvard Apparatus) using a DMZ pipette puller (Zeitz). Pipettes were filled with an intracellular solution containing 105 mM K-gluconate, 10 mM HEPES, 10 mM phosphocreatine-Na, 4 mM ATP-

Na₂, and 30 mM KCl (pH 7.25, adjusted with KOH). The input resistance (R_{input}) was computed using a 10-mV hyperpolarizing step from a holding potential of -65 mV (50 ms). Current-clamp and voltage-clamp recordings were performed using an EPC-10 amplifier (HEKA Elektronik). Data acquisition was performed using Patchmaster software (Heka Elektronik). The liquid junction potential (-5 mV) was left uncorrected. Signals were sampled at 20 kHz and filtered at 4 kHz. Data analysis was performed using Igor Pro (Wavemetrics). Statistical analyses were performed using Prism (GraphPad). The normality of data distribution was tested using Shapiro–Wilk's test. Unpaired two-tailed t-tests (for normally distributed datasets) or Mann–Whitney tests (for non-normally distributed datasets) were used for comparisons between two groups. For multiple comparisons, we used two-way ANOVA followed by Sidak's test. Values of $p < 0.05$ were considered statistically significant.

Quantification And Statistical Analysis

Experimental design and statistical analysis

Statistical analyses were performed using GraphPad Prism 7 software. Starting from our experience in previous publications^{24,29}, we calculated the standard deviation of each group of animals for each test as well as the differences between the means of these groups. By setting the type I and II error risks at 5 and 20%, respectively, the size of the groups were determined by calculating the statistical power using the G*Power software version 3.1.9.6. To ensure reproducibility, when relevant, experiments were performed at least three times independently. To avoid litter bias in the mouse experiments, experimental groups are composed of animals from different litters randomly distributed using Graphpad software. All analyses were conducted with blinding to the experimental condition. Putative outliers were determined by the ROUT method. Data are presented as bars and the line at the mean \pm S.E.M. (standard error of the mean). Comparisons between two groups following a normal distribution were analyzed using two-tailed unpaired t-test with or without Welch's correction. Normality was assessed using the D'Agostino & Pearson omnibus normality test. All data normally distributed for more than two groups were examined by either ordinary two-way ANOVA followed by Tukey's multiple comparisons or repeated measure two-way ANOVA followed by Sidak's multiple comparisons test. Data not passing the normality test were analyzed using the Kruskal-Wallis test followed by Dunn's multiple comparison test. $P < 0.05$ was predetermined as the threshold for statistical significance (See supplementary Table S1 for full statistical analysis).

The supplementary Table S1 provides the full statistical analysis.

ACKNOWLEDGEMENTS

We thank the *Cell and Tissue Imaging Facility* of the Institut du Fer à Moulin (namely Theano Eirinopoulou, Mythili Savariradjane), where all image acquisitions and analyses have been performed, Aude Muzerelle for help with stereotaxic viral injections, and the staff of the IFM animal facility (namely Baptiste Lecomte, Gaël Granec, François Baudoin, Anna-Sophia Lourenço, Emma Courteau and Eloise Marsan).

This work has been supported by grants from the Agence Nationale de la Recherche (ANR-17-CE16-0008, ANR-11-IDEX-0004-02), the Fondation pour la Recherche Médicale (Equipe FRM DEQ2014039529 to L.M and R22184DD to S.L.) and the Fédération pour la Recherche sur le Cerveau (FRC-2019-19F10 to L.M and R20020DD to S.L.).

This manuscript should be distributed under the terms and conditions of the Creative Commons Attribution (CC-BY) license (<https://creativecommons.org/licenses/by/4.0/>).

AUTHOR CONTRIBUTIONS

L.M., S.L., C.L. and A.R. designed the studies. L.M., A.B., C.L and A.R wrote the manuscript, and all authors revised it. A.B., I.M., X.M., and M.R. performed pharmacological studies, BRET experiments, stereotaxy and animal experiments, immunofluorescence, image acquisition and analysis with the help of S.L. C.D. and C.L. performed and analyzed electrophysiological experiments. A.B., S.L., L.M., and A.R. performed data analysis.

DECLARATION OF INTERESTS

The authors declare no conflict of interest.

REFERENCES

1. Arango, V., Huang, Y.-Y., Underwood, M.D., and Mann, J.J. (2003). Genetics of the serotonergic system in suicidal behavior. *J Psy Res* 37, 375-386. 10.1016/s0022-3956(03)00048-7.
2. Mann, J.J. (1999). Role of the serotonergic system in the pathogenesis of major depression and suicidal behavior. *Neuropsychopharm* 21, 99S-105S. 10.1016/S0893-133X(99)00040-8.
3. Marazziti, D. (2017). Understanding the role of serotonin in psychiatric diseases. *F1000Research* 6, 180. 10.12688/f1000research.10094.1.
4. Lin, S.L., Setya, S., Johnson-Farley, N.N., and Cowen, D.S. (2002). Differential coupling of 5-HT(1) receptors to G proteins of the G(i) family. *Br J Pharmacol* 136, 1072-1078. 10.1038/sj.bjp.0704809.
5. Albert, P.R., and Vahid-Ansari, F. (2019). The 5-HT1A receptor: Signaling to behavior. *Biochimie* 161, 34-45. 10.1016/j.biochi.2018.10.015.
6. Andrade, R., Huereca, D., Lyons, J.G., Andrade, E.M., and Mcgregor, K.M. (2015). 5-HT1A Receptor-Mediated Autoinhibition and the Control of Serotonergic Cell Firing. *ACS Chem Neurosci* 6, 1110-1115. 10.1021/acschemneuro.5b00034.
7. Garcia-Garcia, A.L., Newman-Tancredi, A., and Leonardo, E.D. (2014). 5-HT1A receptors in mood and anxiety: recent insights into autoreceptor versus heteroreceptor function. *Psychopharmacology* 231, 623-636. 10.1007/s00213-013-3389-x.
8. McDevitt, R.A., and Neumaier, J.F. (2011). Regulation of dorsal raphe nucleus function by serotonin autoreceptors: a behavioral perspective. *J Chem Neuroanat* 41, 234-246. 10.1016/j.jchemneu.2011.05.001.
9. Courtney, N.A., and Ford, C.P. (2016). Mechanisms of 5-HT1A receptor-mediated transmission in dorsal raphe serotonin neurons. *J Physiol* 594, 953-965. 10.1113/JP271716.
10. Llamas, N., Bruzos-Cidón, C., Rodríguez, J.J., Ugedo, L., and Torrecilla, M. (2015). Deletion of GIRK2 Subunit of GIRK Channels Alters the 5-HT1A Receptor-Mediated Signaling and Results in a Depression-Resistant Behavior. *Int J Neuropsychopharmacol* 18, pyv051. 10.1093/ijnp/pyv051.
11. Montalbano, A., Corradetti, R., and Mlinar, B. (2015). Pharmacological Characterization of 5-HT1A Autoreceptor-Coupled GIRK Channels in Rat Dorsal Raphe 5-HT Neurons. *PLoS One* 10, e0140369. 10.1371/journal.pone.0140369.
12. Heusler, P., Pauwels, P.J., Wurch, T., Newman-Tancredi, A., Tytgat, J., Colpaert, F.C., and Cussac, D. (2005). Differential ion current activation by human 5-HT(1A) receptors in *Xenopus* oocytes: evidence for agonist-directed trafficking of receptor signalling. *Neuropharmacology* 49, 963-976. 10.1016/j.neuropharm.2005.05.001.
13. Kirby, L.G., Pernar, L., Valentino, R.J., and Beck, S.G. (2003). Distinguishing characteristics of serotonin and non-serotonin-containing cells in the dorsal raphe nucleus: electrophysiological and immunohistochemical studies. *Neuroscience* 116, 669-683.
14. Crespi, F. (2009). Apamin increases 5-HT cell firing in raphe dorsalis and extracellular 5-HT levels in amygdala: a concomitant in vivo study in anesthetized rats. *Brain Research* 1281, 35-46. 10.1016/j.brainres.2009.05.021.
15. Rouchet, N., Waroux, O., Lamy, C., Massotte, L., Scuvée-Moreau, J., Liégeois, J.-F., and Seutin, V. (2008). SK channel blockade promotes burst firing in dorsal raphe serotonergic neurons. *Eur J Neurosci* 28, 1108-1115. 10.1111/j.1460-9568.2008.06430.x.
16. Grunnet, M., Jespersen, T., and Perrier, J.-F. (2004). 5-HT1A receptors modulate small-conductance Ca²⁺-activated K⁺ channels. *J Neurosci Res* 78, 845-854. 10.1002/jnr.20318.
17. Riad, M., Watkins, K.C., Doucet, E., Hamon, M., and Descarries, L. (2001). Agonist-induced internalization of serotonin-1a receptors in the dorsal raphe nucleus (autoreceptors) but not hippocampus (heteroreceptors). *J Neurosci* 21, 8378-8386.
18. Soiza-Reilly, M., Goodfellow, N.M., Lambe, E.K., and Commons, K.G. (2015). Enhanced 5-HT1A receptor-dependent feedback control over dorsal raphe serotonin neurons in the SERT knockout mouse. *Neuropharmacology* 89, 185-192. 10.1016/j.neuropharm.2014.09.017.
19. Bevilacqua, L., Doly, S., Kaprio, J., Yuan, Q., Tikkanen, R., Paunio, T., Zhou, Z., Wedenoja, J., Maroteaux, L., Diaz, S., et al. (2010). A population-specific HTR2B stop codon predisposes to severe impulsivity. *Nature* 468, 1061-1066.
20. Tikkanen, R., Tiihonen, J., Rautiainen, M.R., Paunio, T., Bevilacqua, L., Panarsky, R., Goldman, D., and Virkkunen, M. (2015). Impulsive alcohol-related risk-behavior and emotional dysregulation among individuals with a serotonin 2B receptor stop codon. *Transl Psychiatry* 5, e681. 10.1038/tp.2015.170.

21. Diaz, S.L., Doly, S., Narboux-Nême, N., Fernandez, S., Mazot, P., Banas, S., Boutourlinsky, K., Moutkine, I., Belmer, A., Roumier, A., and Maroteaux, L. (2012). 5-HT_{2B} receptors are required for serotonin-selective antidepressant actions. *Mol Psychiatry* 17, 154-163.
22. Niederkofler, V., Asher, T.E., Okaty, B.W., Rood, B.D., Narayan, A., Hwa, L.S., Beck, S.G., Miczek, K.A., and Dymecki, S.M. (2016). Identification of Serotonergic Neuronal Modules that Affect Aggressive Behavior. *Cell Reports* 17, 1934-1949. 10.1016/j.celrep.2016.10.063.
23. Okaty, B.W., Sturrock, N., Escobedo Lozoya, Y., Chang, Y., Senft, R.A., Lyon, K.A., Alekseyenko, O.V., and Dymecki, S.M. (2020). A single-cell transcriptomic and anatomic atlas of mouse dorsal raphe Pet1 neurons. *eLife* 9, e55523. 10.7554/eLife.55523.
24. Belmer, A., Quentin, E., Diaz, S.L., Guiard, B.P., Fernandez, S.P., Doly, S., Banas, S.M., Pitychoutis, P.M., Moutkine, I., Muzerelle, A., et al. (2018). Positive regulation of raphe serotonin neurons by serotonin 2B receptors. *Neuropsychopharmacology* 43, 1623–1632. 10.1038/s41386-018-0013-0.
25. Kidd, E.J., Garratt, J.C., and Marsden, C.A. (1991). Effects of repeated treatment with 1-(2,5-dimethoxy-4-iodophenyl)-2-aminopropane (DOI) on the autoregulatory control of dorsal raphe 5-HT neuronal firing and cortical 5-HT release. *Eur J Pharmacol* 200, 131-139.
26. Maroteaux, L., Béchade, C., and Roumier, A. (2019). Dimers of serotonin receptors: Impact on ligand affinity and signaling. *Biochimie* 161, 22-33. 10.1016/j.biochi.2019.01.009.
27. Moutkine, I., Quentin, E., Guiard, B.P., Maroteaux, L., and Doly, S. (2017). Heterodimers of serotonin receptor subtypes 2 are driven by 5-HT_{2C} protomers. *J Biol Chem* 292, 6352-6368. 10.1074/jbc.M117.779041.
28. Fagni, L., Worley, P.F., and Ango, F. (2002). Homer as both a scaffold and transduction molecule. *Science's STKE* 2002, re8. 10.1126/stke.2002.137.re8.
29. Benhadda, A., Quentin, E., Moutkine, I., Chanrion, B., Russeau, M., Marin, P., Levi, S., and Maroteaux, L. (2021). Serotonin 2B Receptor by Interacting with NMDA Receptor and CIPP Protein Complex May Control Structural Plasticity at Glutamatergic Synapses. *ACS Chem Neurosci* 12, 1133-1149. 10.1021/acschemneuro.0c00638.
30. Kia, H.K., Miquel, M.C., Brisorgueil, M.J., Daval, G., Riad, M., el Mestikawy, S., Hamon, M., and Vergé, D. (1996). Immunocytochemical localization of serotonin_{1A} receptors in the rat central nervous system. *J Comp Neurol* 365, 289-305. 10.1002/(SICI)1096-9861(19960205)365:2<289::AID-CNE7>3.0.CO;2-1.
31. Riad, M., Garcia, S., Watkins, K.C., Jodoin, N., Doucet, E., Langlois, X., el Mestikawy, S., Hamon, M., and Descarries, L. (2000). Somatodendritic localization of 5-HT_{1A} and preterminal axonal localization of 5-HT_{1B} serotonin receptors in adult rat brain. *J Comp Neurol* 417, 181-194.
32. Renner, U., Zeug, A., Woehler, A., Niebert, M., Dityatev, A., Dityateva, G., Gorinski, N., Guseva, D., Abdel-Galil, D., Frohlich, M., et al. (2012). Heterodimerization of serotonin receptors 5-HT_{1A} and 5-HT₇ differentially regulates receptor signalling and trafficking. *J Cell Science* 125, 2486-2499. 10.1242/jcs.101337.
33. Calebiro, D., Koszegi, Z., Lanoiselée, Y., Miljus, T., and O'Brien, S. (2021). G protein-coupled receptor-G protein interactions: a single-molecule perspective. *Physiological reviews* 101, 857-906. 10.1152/physrev.00021.2020.
34. Bouaziz, E., Emerit, M.B., Vodjdani, G., Gautheron, V., Hamon, M., Darmon, M., and Masson, J. (2014). Neuronal phenotype dependency of agonist-induced internalization of the 5-HT_{1A} serotonin receptor. *J Neurosci* 34, 282-294. 10.1523/JNEUROSCI.0186-13.2014.
35. Raymond, J.R., Mukhin, Y.V., Gettys, T.W., and Garnovskaya, M.N. (1999). The recombinant 5-HT_{1A} receptor: G protein coupling and signalling pathways. *Brit J Pharmacol* 127, 1751-1764. 10.1038/sj.bjp.0702723.
36. Heusler, P., Newman-Tancredi, A., Loock, T., and Cussac, D. (2008). Antipsychotics differ in their ability to internalise human dopamine D_{2S} and human serotonin 5-HT_{1A} receptors in HEK293 cells. *Eur J Pharmacol* 581, 37-46. 10.1016/j.ejphar.2007.11.046.
37. Della Rocca, G.J., Maudsley, S., Daaka, Y., Lefkowitz, R.J., and Luttrell, L.M. (1999). Pleiotropic coupling of G protein-coupled receptors to the mitogen-activated protein kinase cascade. Role of focal adhesions and receptor tyrosine kinases. *J Biol Chem* 274, 13978-13984.
38. Janoshazi, A., Deraet, M., Callebert, J., Setola, V., Guenther, S., Saubamea, B., Manivet, P., Launay, J.M., and Maroteaux, L. (2007). Modified receptor internalization upon co-expression of 5-HT_{1B} receptor and 5-HT_{2B} receptors. *Mol Pharmacol* 71, 1463-1474.
39. Herrick-Davis, K. (2013). Functional significance of serotonin receptor dimerization. *Exp Br Res* 230, 375-386. 10.1007/s00221-013-3622-1.

40. Faron-Górecka, A., Szlachta, M., Kolasa, M., Solich, J., Górecki, A., Kuśmider, M., Żurawek, D., and Dziedzicka-Wasylewska, M. (2019). Understanding GPCR dimerization. In *Receptor-Receptor Interactions*, pp. 155-178. 10.1016/bs.mcb.2018.08.005.
41. Borroto-Escuela, D.O., Li, X., Tarakanov, A.O., Savelli, D., Narváez, M., Shumilov, K., Andrade-Talavera, Y., Jimenez-Beristain, A., Pomierny, B., Díaz-Cabiale, Z., et al. (2017). Existence of brain 5-HT_{1A}-5-HT_{2A} isoreceptor complexes with antagonistic allosteric receptor-receptor interactions regulating 5-HT_{1A} receptor recognition. *ACS Omega* 2, 4779-4789. 10.1021/acsomega.7b00629.
42. Avesar, D., and Gullledge, A.T. (2012). Selective serotonergic excitation of callosal projection neurons. *Frontiers in Neural Circuits* 6, 1-11. 10.3389/fncir.2012.00012.
43. Ju, A., Fernandez-Arroyo, B., Wu, Y., Jacky, D., and Beyeler, A. (2020). Expression of serotonin 1A and 2A receptors in molecular- and projection-defined neurons of the mouse insular cortex. *Molecular Brain* 13, 99. 10.1186/s13041-020-00605-5.
44. Llamas, N., Ugedo, L., and Torrecilla, M. (2017). Inactivation of GIRK channels weakens the pre- and postsynaptic inhibitory activity in dorsal raphe neurons. *Physiol Rep* 5, 1-18. 10.14814/phy2.13141.
45. Crespi, F. (2010). SK channel blocker apamin attenuates the effect of SSRI fluoxetine upon cell firing in dorsal raphe nucleus: a concomitant electrophysiological and electrochemical in vivo study reveals implications for modulating extracellular 5-HT. *Brain Research* 1334, 1-11. 10.1016/j.brainres.2010.03.081.
46. Diaz, S.L., Narboux-Nême, N., Boutourlinsky, K., Doly, S., and Maroteaux, L. (2016). Mice lacking the serotonin 5-HT_{2B} receptor as an animal model of resistance to selective serotonin reuptake inhibitors antidepressants. *Eur Neuropsychopharmacol* 26, 265-279. 10.1016/j.euroneuro.2015.12.012.
47. Sargin, D., Oliver, D.K., and Lambe, E.K. (2016). Chronic social isolation reduces 5-HT neuronal activity via upregulated SK3 calcium-activated potassium channels. *eLife* 5, e21416. 10.7554/eLife.21416.
48. Scott, M.M., Wylie, C.J., Lerch, J.K., Murphy, R., Lobur, K., Herlitze, S., Jiang, W., Conlon, R.A., Strowbridge, B.W., and Deneris, E.S. (2005). A genetic approach to access serotonin neurons for in vivo and in vitro studies. *Proc Natl Acad Sci USA* 102, 16472-16477. 0504510102 [pii] 10.1073/pnas.0504510102.
49. Percie du Sert, N., Hurst, V., Ahluwalia, A., Alam, S., Avey, M.T., Baker, M., Browne, W.J., Clark, A., Cuthill, I.C., Dirnagl, U., et al. (2020). The ARRIVE guidelines 2.0: Updated guidelines for reporting animal research. *PLoS Biol* 18, e3000410. 10.1371/journal.pbio.3000410.
50. Muzerelle, A., Scotto-Lomassese, S., Bernard, J.F., Soiza-Reilly, M., and Gaspar, P. (2016). Conditional anterograde tracing reveals distinct targeting of individual serotonin cell groups (B5-B9) to the forebrain and brainstem. *Br Struct Function* 221, 535-561. 10.1007/s00429-014-0924-4.
51. Bolte, S., and Cordelières, F.P. (2006). A guided tour into subcellular colocalization analysis in light microscopy. *J Microscopy* 224, 213-232. 10.1111/j.1365-2818.2006.01706.x.
52. Kumar, G.A., Sarkar, P., Jafurulla, M., Singh, S.P., Srinivas, G., Pande, G., and Chattopadhyay, A. (2019). Exploring Endocytosis and Intracellular Trafficking of the Human Serotonin_{1A} Receptor. *Biochemistry* 58, 2628-2641. 10.1021/acs.biochem.9b00033.
53. Specht, C.G., Izeddin, I., Rodriguez, P.C., El Beheiry, M., Rostaing, P., Darzacq, X., Dahan, M., and Triller, A. (2013). Quantitative nanoscopy of inhibitory synapses: counting gephyrin molecules and receptor binding sites. *Neuron* 79, 308-321. 10.1016/j.neuron.2013.05.013.

FIGURES LEGENDS

Figure 1: Physical proximity of 5-HT_{2B} and 5-HT_{1A} in transfected cells does not affect second messenger signaling. (A) Co-immunoprecipitation of 5-HT_{1A} with 5-HT_{2B} in COS-7 cells. Proteins from COS-7 cells co-transfected with plasmids coding for HA-tagged 5-HT_{2B} (HA-5-HT_{2B}) and myc-tagged 5-HT_{1A} (myc-5-HT_{1A}) were immunoprecipitated with an anti-HA antibody and analyzed by anti-HA (top) or anti-myc (bottom) Western-blotting. Western-blots on the whole extract (“input”) show the presence of the receptors in each condition (Input; left panel). Immunoprecipitations using anti-HA beads (IP-HA; right panel) reveal a co-immunoprecipitation between 5-HT_{1A} and 5-HT_{2B}. Molecular weight marker of 50 Kd (M). (B) BRET proximity assays for 5-HT_{1A} and 5-HT_{2B}. COS-7 cells were co-transfected with a constant amount of plasmid coding for 5-HT_{2B}-RLuc (BRET donor) and increasing amounts of plasmid encoding YFP-tagged 5-HT_{1A} (5-HT_{1A}-YFP BRET acceptor) or YFP-tagged 5-HT_{2B} (5-HT_{2B}-YFP) as negative control unable to form dimers²⁷. The hyperbolic curve attests close interaction between 5-HT_{1A}-YFP and 5-HT_{2B}-RLuc with a physical distance <10 nm (representative experiment of n > 3 independent experiments). (C-H) Pharmacological characterization of co-expressed receptors. Radioligand binding competition by BW or NAN of tritiated-mesulergine (C-D) or 8-OH-DPAT (E-F) performed on whole membrane proteins from transfected COS-7 cells expressing 5-HT_{2B} with or without 5-HT_{1A}. Coexpression of 5-HT_{2B} with 5-HT_{1A} did not modify the binding affinity to their respective ligand (K_i) compared to single 5-HT_{2B} expression. Data were analyzed using the Mann-Whitney unpaired t-test. Representative curves of n = 3 independent experiments, each performed in duplicate. (G-H) Impact of coexpression on 5-HT_{2B}- and 5-HT_{1A}-operated signal transduction. The quantification of inositol phosphate was performed in COS-7 cells expressing 5-HT_{2B} with or without 5-HT_{1A} and stimulated with increasing concentrations of the 5-HT_{2B} agonist BW. Note the absence of effect, in the coexpression of 5-HT_{2B} with 5-HT_{1A}, on IP production compared to the single 5-HT_{2B} expression condition. Data were statistically analyzed by Mann-Whitney unpaired t-test. Representative curves of n = 3 independent experiments, each performed in duplicate. Individual values are presented with mean ± SEM

Figure 2: 5-HT_{2B} /5-HT_{1A} co-expression decreases 5-HT_{2B} plasma membrane expression. (A). Radioligand binding competition by BW of tritiated mesulergine performed on membrane proteins of intact (non-permeabilized) COS-7 cells transfected to express 5-HT_{2B} alone or with 5-HT_{1A}. (B) Co-expression decreases membrane expression of 5-HT_{2B}, as illustrated by a significant decrease in B_{max} (p=0.0336). Data were analyzed using unpaired t-test with Welch's correction; n = 3 independent experiments, each performed in duplicate. (C-E). Surface biotinylation performed on COS-7 cells expressing 5-HT_{1A} and/or 5-HT_{2B}. (C) Analysis by Western blotting. (D-E). Ratio of the membrane/total protein levels for each receptor analyzed in conditions of simple or co-expression. Co-expression of the two receptors limits the proportion of 5-HT_{2B} (unpaired t-test p=0.0477, n = 5) but not 5-HT_{1A} (unpaired t-test p=0.3834, n=5) reaching the plasma membrane. Representative curves of n = 5 independent experiments. Band intensity of each condition was quantified and represented graphically. (*p<0,05). Individual values are presented with mean ± SEM

Figure 3: Co-expression of 5-HT_{2B} with 5-HT_{1A} in hippocampal neurons increases 5-HT_{2B} membrane clustering and maintains 5-HT_{1A} surface expression upon selective agonist stimulation. (A). 5-HT_{2B} localization by HA-tag immunostaining (red) revealed

receptor clustering at the dendritic membrane of hippocampal neurons, whereas 5-HT_{1A} localization studied by myc-tag immunostaining (green) revealed a more even distribution in smaller clusters, which are in part colocalized with 5-HT_{2B} clusters (white arrows). **(B)**. Quantification of the staining intensities in the absence (plasma membrane expression) or in the presence (total expression) of detergent indicates that co-expressing 5-HT_{1A} with 5-HT_{2B} decreases the membrane/total ratio of 5-HT_{2B} (values normalized to the ratio in 5-HT_{2B} single transfection condition, $p=0.0084$, as assessed by unpaired t-test; $n=20-24$ dendrites from 3 independent cell cultures; Scale bars, 5 μm). **(C)**. 5-HT_{2B} clustering at the dendritic membrane 0, 10 or 20 min after BW stimulation in the absence (top) or presence (bottom) of 5-HT_{1A}. Scale bars, 10 μm . **(D)**, Quantification of 5-HT_{2B} membrane clustering following agonist stimulation in the presence (or not) of 5-HT_{1A}. Upon 5-HT_{2B} stimulation by BW (1 μM), the number of 5-HT_{2B} clusters decreased in the absence of 5-HT_{1A} ($p=0.0026$ t0 vs. t10 and $p < 0.0001$ t0 vs. t20), as revealed by Kruskal-Wallis test, $P < 0.0001$, followed by Dunn's multiple comparisons test; in the presence of 5-HT_{1A}, the 5-HT_{2B} cluster number decreased in the absence of BW stimulation and was unaffected by BW stimulation, $p=0.004$ t0 5-HT_{2B} vs. t0 5-HT_{1A}. The BW stimulation of 5-HT_{2B} alone increased the cluster size (area), $p=0.0016$ t0 vs. t10 and $p < 0.0001$ t0 vs. t20; in the presence of 5-HT_{1A}, the 5-HT_{2B} cluster area increased but was unaffected by BW stimulation, $p=0.0008$ t0 5-HT_{2B} vs. t0 5-HT_{1A}. The BW stimulation slightly increased the molecular density of clusters (integrated intensity) of 5-HT_{2B} clusters from 0 to 20 min in the absence of 5-HT_{1A}, $p=0.00007$ t0 vs. t20; in the presence of 5-HT_{1A}, the 5-HT_{2B} cluster integrated intensity was unaffected without or with BW stimulation. $n = 19-38$ dendrites from 3-4 independent cell cultures. **(E)**. 5-HT_{1A} expression at the dendritic membrane 0, 10 or 20 min after 8-OH-DPAT stimulation in the absence (top) or presence (bottom) of 5-HT_{2B}. Scale bars, 10 μm . **(F)**, Quantification of 5-HT_{1A} membrane expression following agonist stimulation in the presence (or not) of 5-HT_{2B}. Upon 5-HT_{1A} stimulation by 8-OH-DPAT (1 μM), 5-HT_{1A} expression at the neuronal membrane decreased from 0 to 10 min in the absence of 5-HT_{2B} compared to t0 as revealed by Kruskal-Wallis test, $P < 0.0001$, followed by Dunn's multiple comparisons test, $p=0.0115$ t0 vs. t10; in the presence of 5-HT_{2B}, the 5-HT_{1A} expression increased but was unaffected by 8-OH-DPAT stimulation, $p=0.0172$ t0 5-HT_{2B} vs. t0 5-HT_{1A}+5-HT_{2B}. $n = 18-43$ dendrites from 3 independent cell cultures. In all graphs, data, expressed as percentage of their respective values at t0. **** $p < 0.0001$, *** $p < 0.001$, ** $p < 0.01$, * $p < 0.05$. Individual values are presented with mean \pm SEM.

Figure 4: Super-resolution microscopy fully validates that co-expression of 5-HT_{2B} with 5-HT_{1A} increases 5-HT_{2B} membrane clustering as upon BW agonist stimulation. **(A)**. (Top) Images of 5-HT_{2B} membrane clusters acquired by epifluorescence microscopy. Note that clusters are not well-defined and diffuse compared to the lower images acquired at super resolution. Scale bar, 5 μm . (Middle and Bottom). STORM images of 5-HT_{2B} obtained from the dendritic regions shown in A before (left panel) or 20 min (right panel) after BW stimulation in the absence (middle) or presence (bottom) of 5-HT_{1A}. Scale bars, 5 μm . **(B)**. Quantification of 5-HT_{2B} clustering following agonist stimulation in the presence or not of 5-HT_{1A}. The number of 5-HT_{2B} clusters was significantly decreased upon stimulation by BW (1 μM) or by co-expression with 5-HT_{1A}. Two-way ANOVA revealed main effects of agonist treatment $F_{1, 70} = 11.15$, $P=0.0014$ and receptor expression $F_{1, 70} = 25.31$, $P < 0.0001$; t0 5-HT_{2B} vs. t0 5-HT_{2B}+5-HT_{1A} $p= 0.0004$; t20 5-HT_{2B} vs. t20 5-HT_{2B}+5-HT_{1A} $p= 0.028$; t0 vs. t20 5-HT_{2B}, $p=0.0271$ by Tukey's multiple comparisons test. The area of 5-HT_{2B} clusters was significantly increased upon stimulation by BW for 20 min (t20) or by co-expression with 5-HT_{1A}. Two-way ANOVA revealed main effects of agonist treatment $F_{1, 70} = 7.067$, $P=0.0097$

and receptor expression $F_{1,70} = 16.78$, $P=0.0001$; t_0 5-HT_{2B} vs. t_0 5-HT_{2B}+5-HT_{1A} $p= 0.0402$; t_{20} 5-HT_{2B} vs. t_{20} 5-HT_{2B}+5-HT_{1A} $p= 0.0156$ by Tukey's multiple comparisons test. $n = 16-21$ dendrites from 3 independent cell cultures. Data are expressed as percentage of their respective values at t_0 . **** $p<0.0001$, *** $p<0.001$, ** $p < 0.01$, * $p < 0.05$. Bars and error bars represent mean \pm SEM.

Figure 5: Cross-stimulation of 5-HT_{2B} or 5-HT_{1A} affects their respective membrane expression. (A). Images of 5-HT_{1A} membrane expression acquired by confocal microscopy. 5-HT_{1A} (green) in the absence (top) or presence of 5-HT_{2B}, (bottom) before or 20 min after BW stimulation. Scale bar, 10 μ m. (B) Quantification of 5-HT_{1A} membrane expression in neurons expressing 5-HT_{1A} alone or in combination with 5-HT_{2B}, with or without 5-HT_{2B} stimulation by BW (1 μ M). One-way ANOVA analysis shows a significant effect of the co-expression of 5-HT_{2B} $F_{2,43} = 16.15$, $P<0.0001$, with an increase in 5-HT_{1A} membrane expression, as shown by Tukey's multiple comparison ($p=0.0188$ vs. non-stimulated 5-HT_{1A}); the 5-HT_{2B} stimulation by BW in co-expression experiment abolishes this effect ($p<0.0001$ vs. non-stimulated) and even reverses this effect ($p=0.0463$) as compared to non-stimulated neurons expressing 5-HT_{1A} alone. $n = 12-22$ dendrites from 2 independent cell cultures. (C) Images of 5-HT_{2B} membrane expression acquired by confocal microscopy. 5-HT_{2B} (red) clustering at the dendritic membrane before or after 8-OH-DPAT stimulation (t_{20} , 20 min) in the presence of 5-HT_{1A}. Scale bar, 10 μ m. (D-F) Quantification of 5-HT_{2B} clustering in neurons co-expressing 5-HT_{1A} in control condition or after 10 or 20 min of 5-HT_{1A} stimulation with 8-OH-DPAT (1 μ M). (D) Upon stimulation by 8-OH-DPAT, the number of 5-HT_{2B} clusters decreased as revealed by Kruskal-Wallis test, $P<0.0001$, followed by Dunn's multiple comparisons test; $p<0.0001$ t_0 vs. t_{10} and $p=0.0001$ t_0 vs. t_{20} ; (E) their area was increased, as revealed by Kruskal-Wallis test, $P<0.0001$, followed by Dunn's multiple comparisons test, $p<0.0001$, t_0 vs. t_{10} and $p<0.0001$ t_0 vs. t_{20} ; (F) their molecular density (integrated intensity) was also increased, as revealed by Kruskal-Wallis test, $P<0.0001$, followed by Dunn's multiple comparisons test, $p<0.0001$ t_0 vs. t_{10} and $p<0.0001$ t_0 vs. t_{20} . Data are expressed as percentage of their respective values at t_0 . $n = 11-24$ dendrites from 3 independent cell cultures. **** $p<0.0001$, *** $p<0.001$, ** $p < 0.01$, * $p < 0.05$. Individual values are presented with mean \pm SEM

Figure 6: 5-HT stimulation of 5-HT_{1A} and 5-HT_{2B} expressed separately or in combination differentially affects their membrane expression and clustering. (A). Quantification of 5-HT_{2B} membrane clustering following 5-HT stimulation in the presence or not of 5-HT_{1A}. In the presence of 5-HT_{1A}, the number of 5-HT_{2B} clusters decreased as revealed by Kruskal-Wallis test, $P<0.0001$, followed by Dunn's multiple comparisons test; $p<0.0001$, t_0 5-HT_{2B} vs. t_0 5-HT_{1A}+5-HT_{2B} and $p<0.0001$, t_0 5-HT_{2B} vs. t_{20} 5-HT_{1A}+5-HT_{2B}, but 5-HT_{2B} clustering was unaffected upon 5-HT (1 μ M) stimulation. In the presence of 5-HT_{1A}, 5-HT_{2B} cluster area increased, as revealed by Kruskal-Wallis test, $P<0.0001$, followed by Dunn's multiple comparisons test, $p<0.0001$, t_0 5-HT_{2B} vs. t_0 5-HT_{1A}+5-HT_{2B} and $p<0.0001$, t_0 5-HT_{2B} vs. t_{20} 5-HT_{1A}+5-HT_{2B}, but was unaffected upon 5-HT stimulation; their molecular density (integrated intensity) was not modified by 5-HT stimulation from 0 to 20 min in the absence or presence of 5-HT_{1A}. Data are expressed as percentage of their respective values at t_0 . ($n = 30-39$ dendrites from 4 independent cell cultures). (B). Images of 5-HT_{1A} membrane expression acquired by confocal microscopy. Top, 5-HT_{1A} (green) expression at the dendritic membrane in the absence of 5-HT_{2B} and before or 20 min after 5-HT stimulation. Bottom, 5-HT_{1A} expression at the dendritic membrane in the presence of 5-

HT_{2B} and before, 20 min after 5-HT stimulation (1 μ M) or 20 min after 5-HT stimulation in the presence of the 5-HT_{2B} antagonist RS (1 μ M). Scale bar, 10 μ m. (C). Quantification of 5-HT_{1A} membrane expression after 5-HT stimulation in the absence or presence of 5-HT_{2B}. The intensity of 5-HT_{1A} at the neuronal membrane was decreased by 5-HT stimulation as revealed by Kruskal-Wallis test, $P < 0.0001$, followed by Dunn's multiple comparisons test, $p = 0.0003$, t0 5-HT_{1A} vs. t20 5-HT_{1A}. Similarly, in the presence of 5-HT_{2B}, the 5-HT_{1A} membrane expression was decreased upon 5-HT stimulation, $p < 0.0001$, t0 5-HT_{1A}+5-HT_{2B} vs. t20 5-HT_{1A}+5-HT_{2B}, but remained unaffected upon 5-HT stimulation in the presence of 5-HT_{2B} antagonist RS. $n = 27-50$ dendrites from 4 independent cell cultures. Data are expressed as percentage of their respective values at t0. **** $p < 0.0001$, *** $p < 0.001$, ** $p < 0.01$, * $p < 0.05$. Individual values are presented with mean \pm SEM.

Figure 7: Colocalization of 5-HT_{1A} and 5-HT_{2B} in somatodendritic compartment of 5-HT neurons and co-regulation of their firing activity through SK channels. (A). Schematic of AAVs injection in B7 raphe nucleus from Pet1-GFP mice, to overexpress HA-5-HT_{2B} and FLAG-5-HT_{1A} into 5-HT neuron. Left: map of DIO-AAV construct that allows Cre-mediated expression of the tagged receptor. Right AAV-DIO-HA5-HT_{2B} and AAV-DIO-FLAG5-HT_{1A} were unilaterally co-injected into B7 raphe nucleus of Pet1-GFP mice to expressed both receptors specifically in dorsal raphe 5-HT neurons. (B). Mouse brainstem sections were examined to assess the distribution of FLAG-tagged 5-HT_{1A} and HA-tagged 5-HT_{2B} expressed specifically in 5-HT neurons. Images of dorsal raphe 5-HT neurons labeled with anti-Flag (green) and anti-HA (red) antibodies, at increasing magnifications (Top and lower panels). (C) Analysis of confocal images taken at higher magnification. Similar colocalization of both receptors was observed in the somatodendritic compartment (Upper right panel). ($n = 6$ images, about 18 cells from 3 independent infections). Scale bars, 100, 40, and 20 μ m, as indicated. (D). Left, sample spike trains evoked by a 400pA current injection in slices from GFP^{5-HT} and 2B-KO^{5-HT}::GFP^{5-HT} mice; scale: 25pA/100ms. Right, F-I curve (mean \pm SEM) for GFP^{5-HT} ($n = 26$ neurons, 1-2 neurons per slice, 3-4 slice from 7 mice) and 2B-KO^{5-HT}::GFP^{5-HT} 5-HT neurons ($n = 27$ neurons, 1-2 neurons per slice, 3-4 slice from 6 mice); two-way RM ANOVA, genotype effect, not significant $p = 0.8715$. (E). Resting membrane potential (V_{rest}) and input resistance in GFP^{5-HT} and 2B-KO^{5-HT}::GFP^{5-HT} 5-HT neurons. Bars represent the mean \pm SEM; circles show individual recordings. (F). Left, same as in (D) in presence of 8-OH-DPAT (30 nM), a 5-HT_{1A} selective agonist. Right, F-I curve (mean \pm SEM) for GFP^{5-HT} ($n = 35$ neurons, 1-2 neurons per slice, 3-4 slice from 5 mice) and 2B-KO^{5-HT}::GFP^{5-HT} 5-HT neurons ($n = 29$ neurons, 1-2 neurons per slice, 3-4 slice from 4 mice) in the presence of 8-OH-DPAT (30 nM); two-way RM ANOVA revealed a significant increase in firing rate of 2B-KO^{5-HT}::GFP^{5-HT}, genotype effect $p < 0.0001$; Sidak's *post hoc* test* $p = 0.0274$, ** $p = 0.0028$, *** $p = 0.0001$, **** $p < 0.0001$. (G) Same as in (E) in the presence of 8-OH-DPAT (30 nM). (H) Left, same as in (D) and (F) in the presence of 8-OH-DPAT (30nM) and Apamin (20 nM), a selective SK channel blocker. Right, F-I curve (mean \pm SEM) for GFP^{5-HT} ($n = 31$ neurons, 1-2 neurons per slice, 3-4 slice from 4 individual mice) and 2B-KO^{5-HT}::GFP^{5-HT} 5-HT neurons ($n = 27$ neurons, 1-2 neurons per slice, 3-4 slice from 3 mice) in the presence of 8-OH-DPAT (30 nM) and Apamin (20 nM); two-way RM ANOVA, no genotype effect $p = 0.6979$. (I) Same as in (D) and (F) in the presence of 8-OH-DPAT (30 nM) and Apamin (20 nM).

Figure 8: Co-expression of 5-HT_{1A} and 5-HT_{2B} impacts their membrane expression, clustering, and physiological function. (A). Separate expression of 5-HT_{1A} or 5-HT_{2B}. Top,

BW stimulation increases 5-HT_{2B} clustering. Bottom, 8-OH-DPAT stimulation decreases membrane expression of 5-HT_{1A} probably via endocytosis. **(B)**. Co-expression of 5-HT_{2B} and 5-HT_{1A} and their stimulation affects the membrane expression of both receptors. Top, 5-HT_{1A} expression increases 5-HT_{2B} clustering. The 5-HT_{2B} stimulation by BW does not reverse the clustering effect of 5-HT_{1A} on 5-HT_{2B}. Stimulation by 8-OH-DPAT of 5-HT_{1A} further increases 5-HT_{2B} clustering. Bottom, Coexpression of 5-HT_{2B} increases 5-HT_{1A} membrane expression. No further change in membrane expression of 5-HT_{1A} is detected upon its stimulation with 8-OH-DPAT, but 5-HT_{2B} stimulation by BW decreases 5-HT_{1A} membrane expression. **(C)**. The 5-HT_{2B}/5-HT_{1A} co-expression/interaction regulates the excitability of 5-HT neurons. In the absence of 5-HT_{2B} (Separated expression, i.e. 2B-KO5-HT, left), 5-HT neuron firing activity is increased upon 5-HT_{1A} stimulation by 8-OH-DPAT, independently of SK channels blockade by apamin. By contrast, upon co-expression of 5-HT_{2B} (Co-expression, i.e. WT, right), 5-HT neuron firing activity is decreased by 8-OH-DPAT unless SK channels are blocked by apamin.

Accumulation of 5-HT_{2B} in cluster is in blue with variations in size and intensity. Membrane association of 5-HT_{1A} in small cluster is in red with internalization at intracellular compartments (Intra). Plasma membrane is in green.

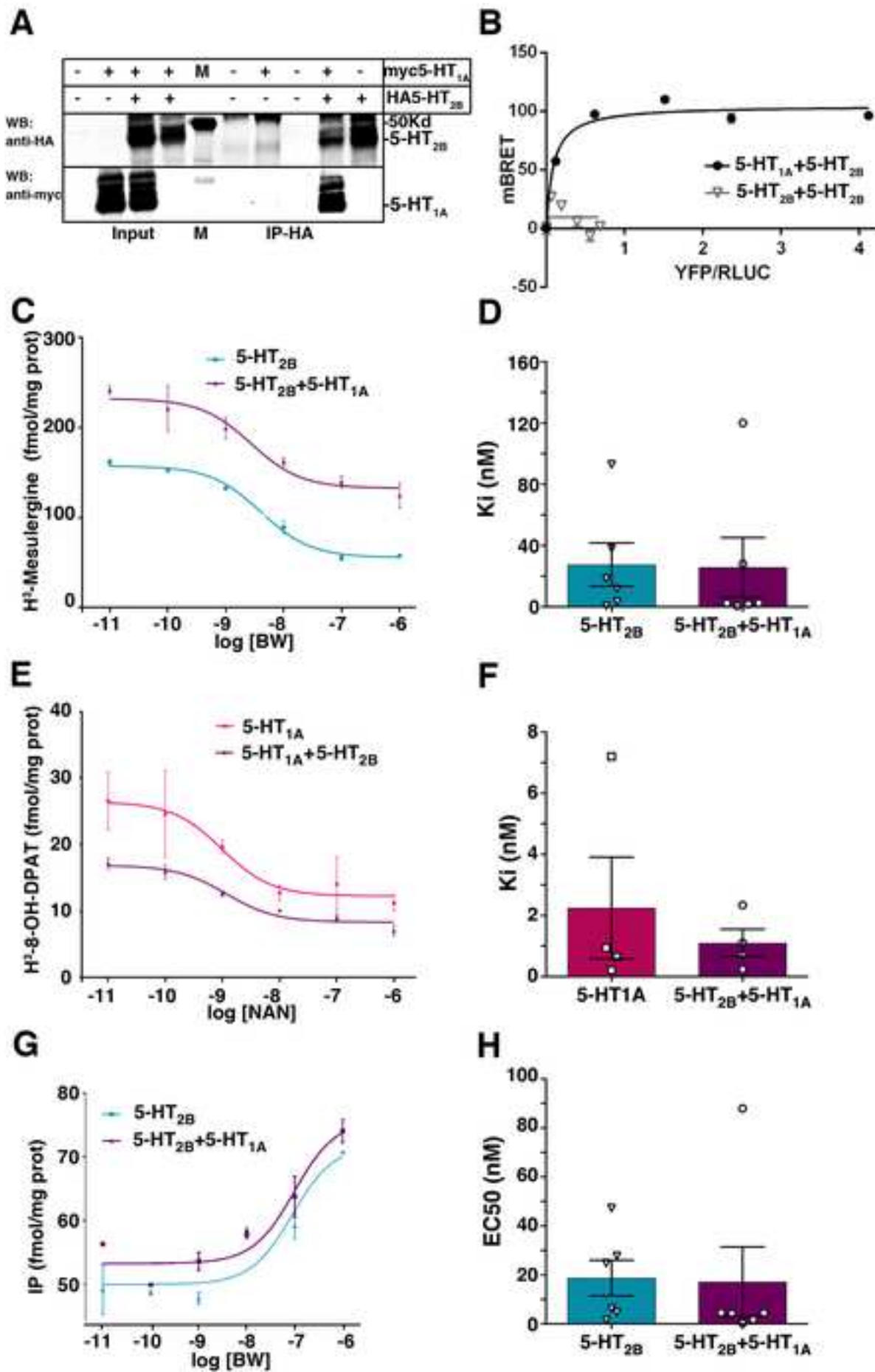
KEY RESOURCES TABLE

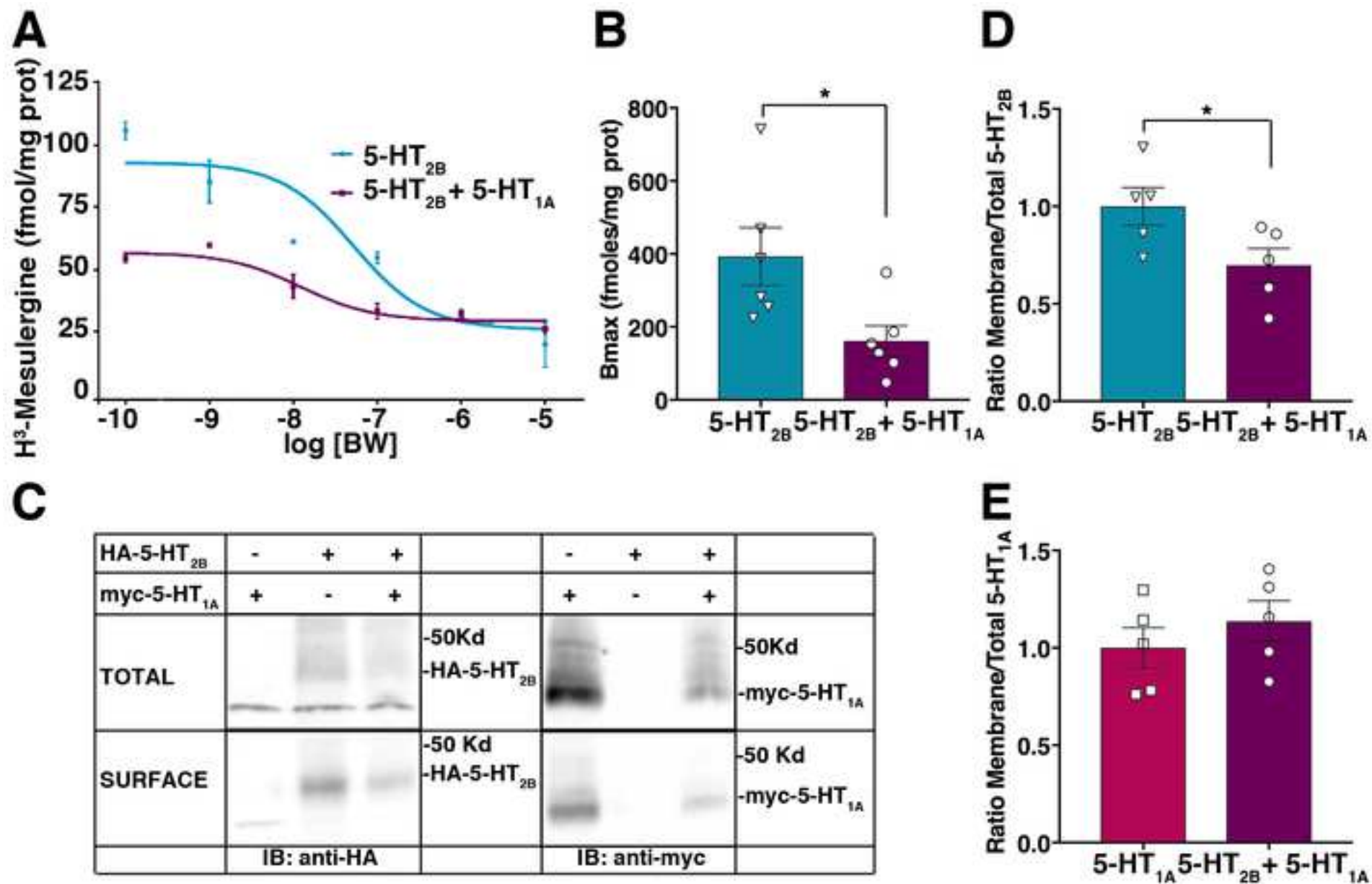
REAGENT or RESOURCE	SOURCE	IDENTIFIER
Antibodies		
mouse anti-HA antibody	Cell Signaling#2367,	RRID AB_10691311
rabbit anti-Flag	Cell Signaling#14793	RRID AB_2572291
Cy5-conjugated donkey anti-mouse	Jackson ImmunoResearch#715-175-150,	RRID AB_2340819
Cy3-conjugated goat anti-rabbit antibody	Jackson ImmunoResearch#111-165-003,	RRID AB_2338000
HA-Tag C29F4 Rabbit mAb Sepharose® Bead Conjugate	Cell Signaling #3956	RRID:AB_10695091
rabbit anti-HA	Cell Signaling#3724,	RRID AB_1549585
mouse anti-myc	Cell Signaling#2276,	RRID AB_331783
goat anti-mouse-IR800	Advansta# R-05060-250	n/a
goat anti-rabbit-IR700	Advansta# R-05054-250	n/a
Alexa 488 donkey anti- mouse antibody	Jackson ImmunoResearch #715-175-150	RRID AB_2336933
Bacterial and virus strains		
pAAV-EF1A-DIO-WPRE-pA vector	(Belmer et al., 2018)	RRID Addgene_39320
Biological samples		
Chemicals, peptides, and recombinant proteins		
³ H-mesulergine	Perkin-Elmer (Belmer et al., 2018)	NET1148250UC
³ H-8-OH-DPAT	ISOBIO	ART-0890
BW-723C86	Tocris	Cat. No. 1059
RS-127445	Tocris	Cat. No. 2993
8-OH-DPAT	Tocris	Cat. No. 0529
NAN-190	Tocris	Cat. No. 0553
Critical commercial assays		
IP one HTRF Kit	Cisbio, France	62IPAPEB
Deposited data		
Experimental models: Cell lines		
COS-7 cells	LGC STANDARDS	ATCC-CRL-1651pCAGG-

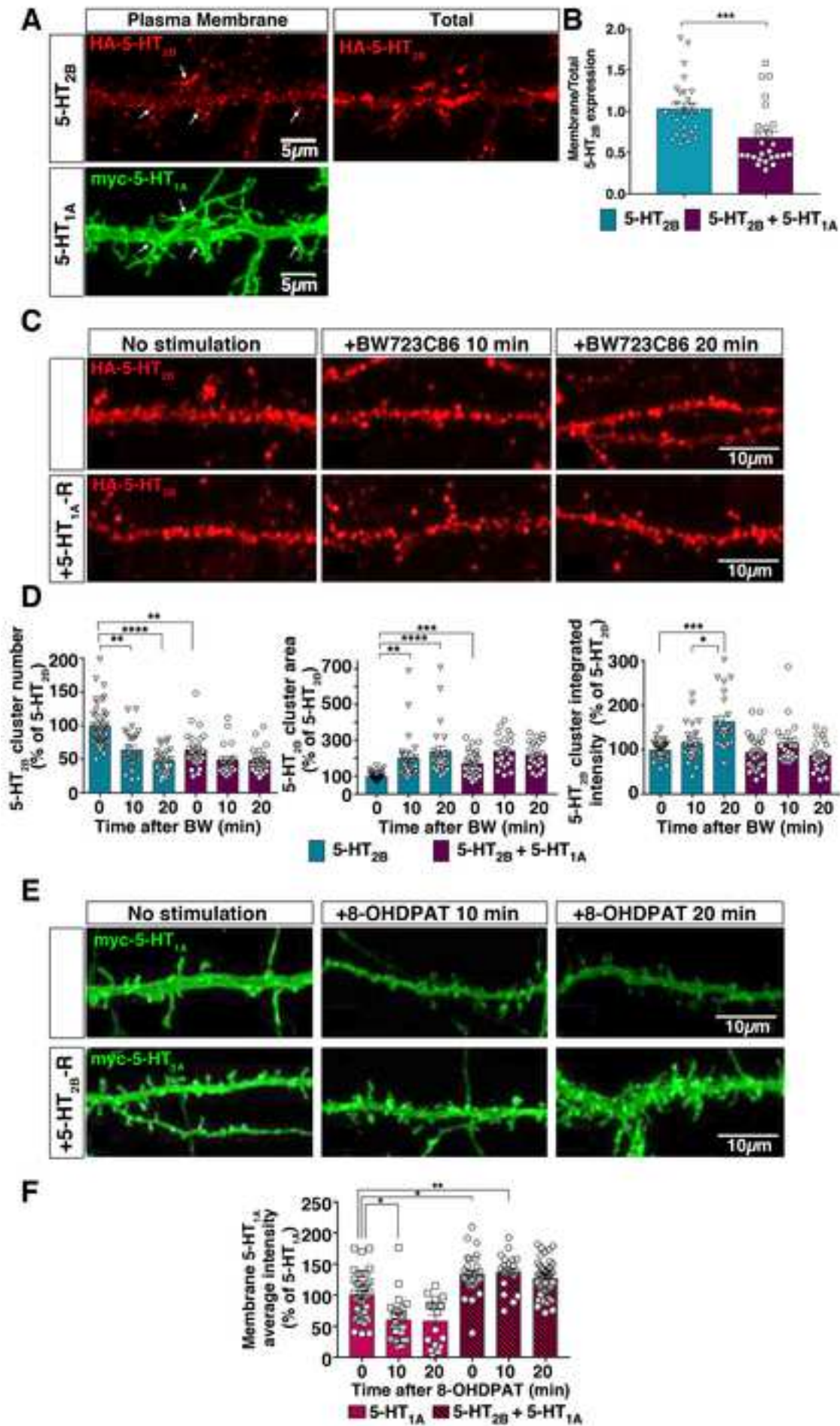
Experimental models: Organisms/strains		
<i>Htr2b^{tm2Lum}/Htr2b^{tm2Lum}</i>	EM:05939, (Belmer et al., 2018)	RRID: IMSR_EM:05939
<i>129S2.Cg-Tg(Fev-cre)^{1Esd}/0</i>	IMSR Cat# JAX:012712, (Scott et al., 2005)	RRID:IMSR_JAX:012712
<i>Gt(ROSA)26Sor^{tm1(CAG-EGFP)Fsh}/Gt(ROSA)26Sor⁺</i>	MGI Cat# 4420760,	RRID:MGI:4420760
Oligonucleotides		
Recombinant DNA		
pCAGG-HA-5-HT _{2B}	(Benhadda et al., 2021)	
pCAGG-myc-5-HT _{1A}	This work	
pCAGG-5-HT _{2B} -R-Rluc	(Moutkine et al., 2017)	
pCAGG-5-HT _{1A} -R-YFP	This work	
pAAV-Flag-5-HT _{1A}	This work	
pAAV-HA-5-HT _{2B}	This work	
pAAV-Ef1a-DIO-VGAT-WPRE-pA	gift from Bernardo Sabatini	RRID: Addgene_39320
Software and algorithms		
ImageJ	(Schneider et al., 2012)	https://imagej.nih.gov/ij/
Other		

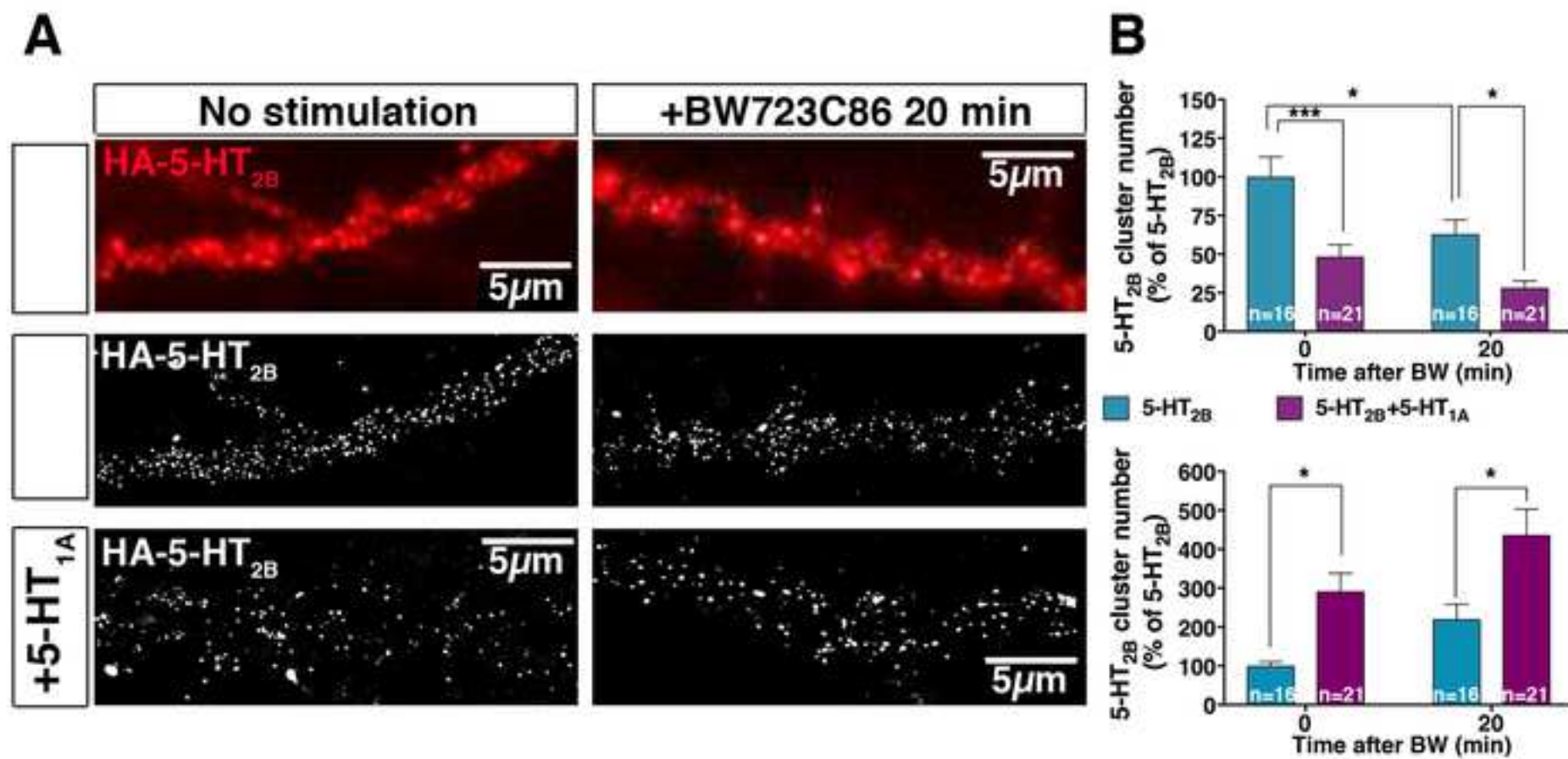
References

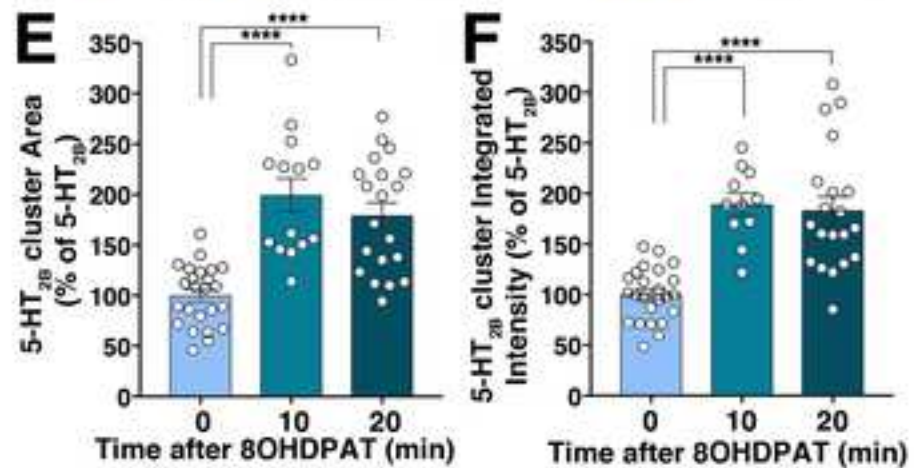
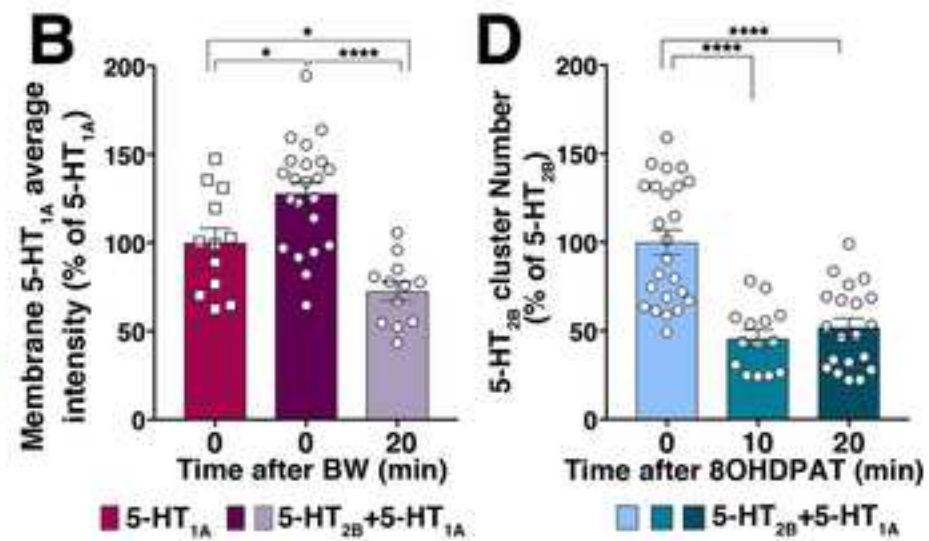
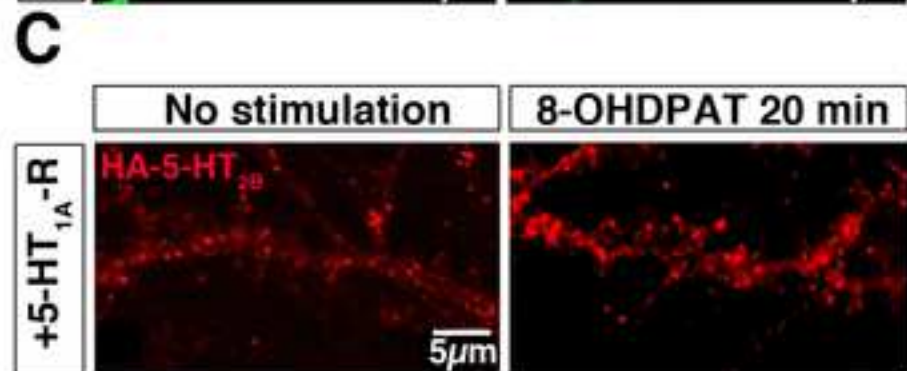
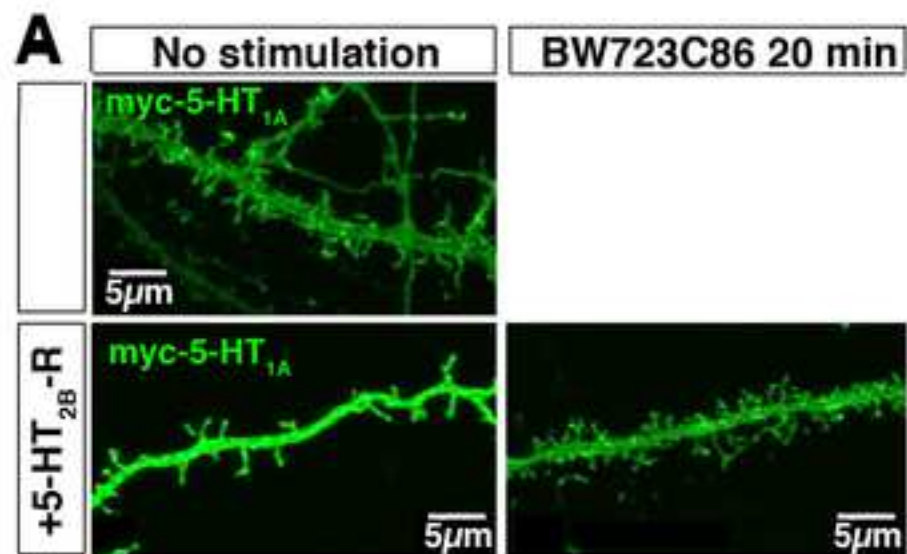
- Belmer, A., et al. (2018). Positive regulation of raphe serotonin neurons by serotonin 2B receptors. *Neuropsychopharmacology* *43*, 1623–1632.
- Benhadda, A., et al. (2021). Serotonin 2B Receptor by Interacting with NMDA Receptor and CIPP Protein Complex May Control Structural Plasticity at Glutamatergic Synapses. *ACS Chem Neurosci* *12*, 1133-1149.
- Moutkine, I., et al. (2017). Heterodimers of serotonin receptor subtypes 2 are driven by 5-HT_{2C} promoters. *J Biol Chem* *292*, 6352-6368.
- Schneider, C.A., et al. (2012). NIH Image to ImageJ: 25 years of image analysis. *Nature methods* *9*, 671-675.
- Scott, M.M., et al. (2005). A genetic approach to access serotonin neurons for in vivo and in vitro studies. *Proc Natl Acad Sci USA* *102*, 16472-16477.

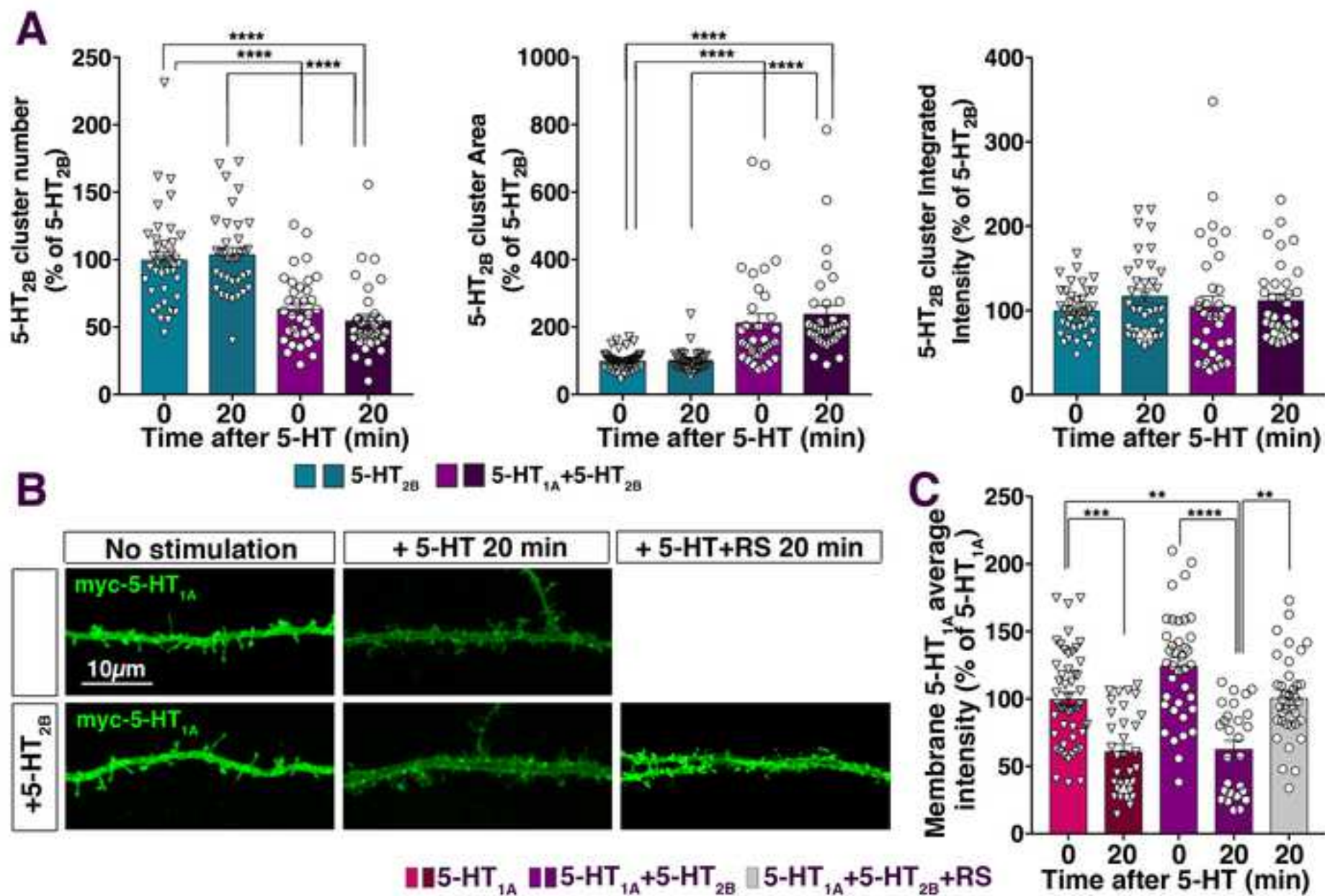


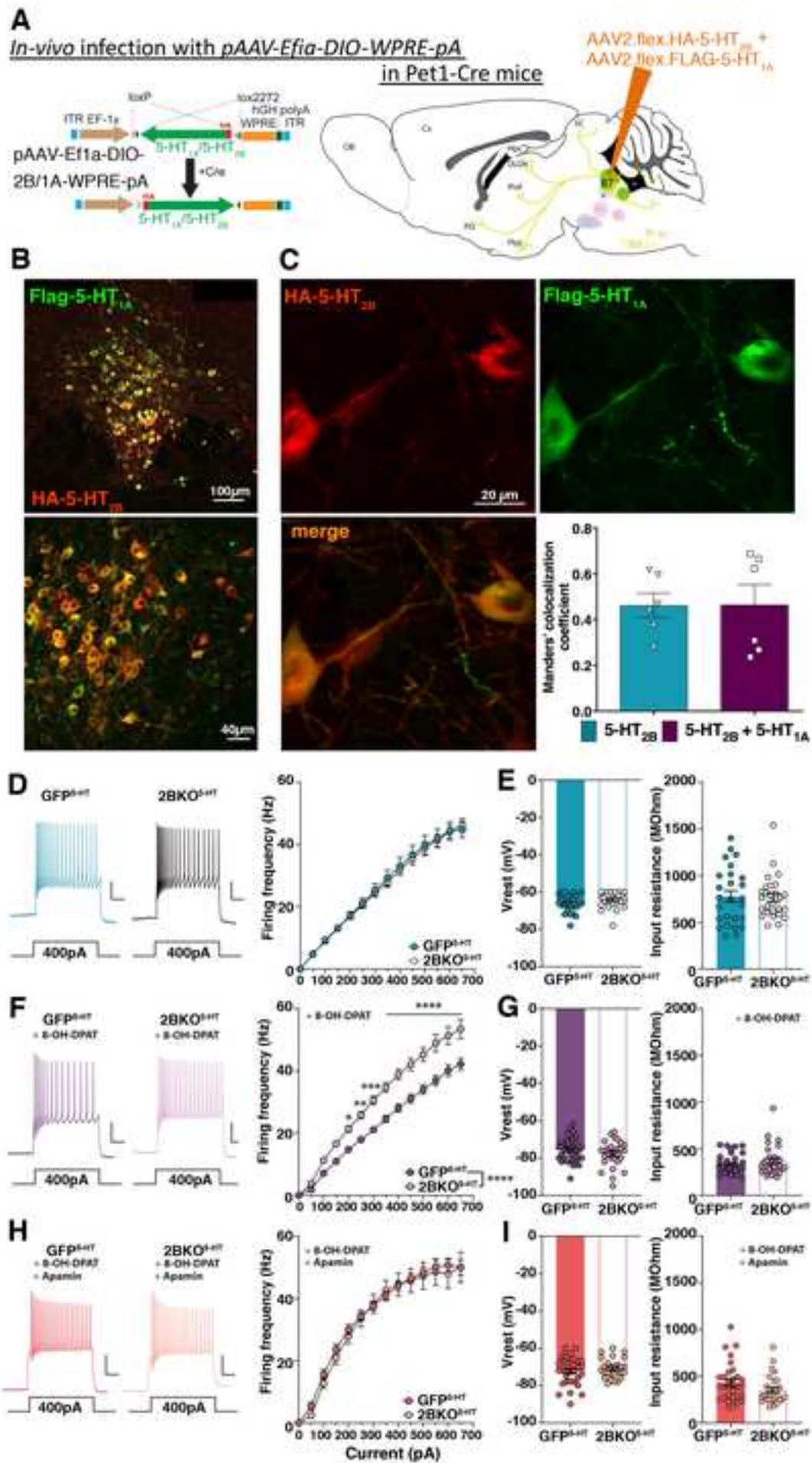












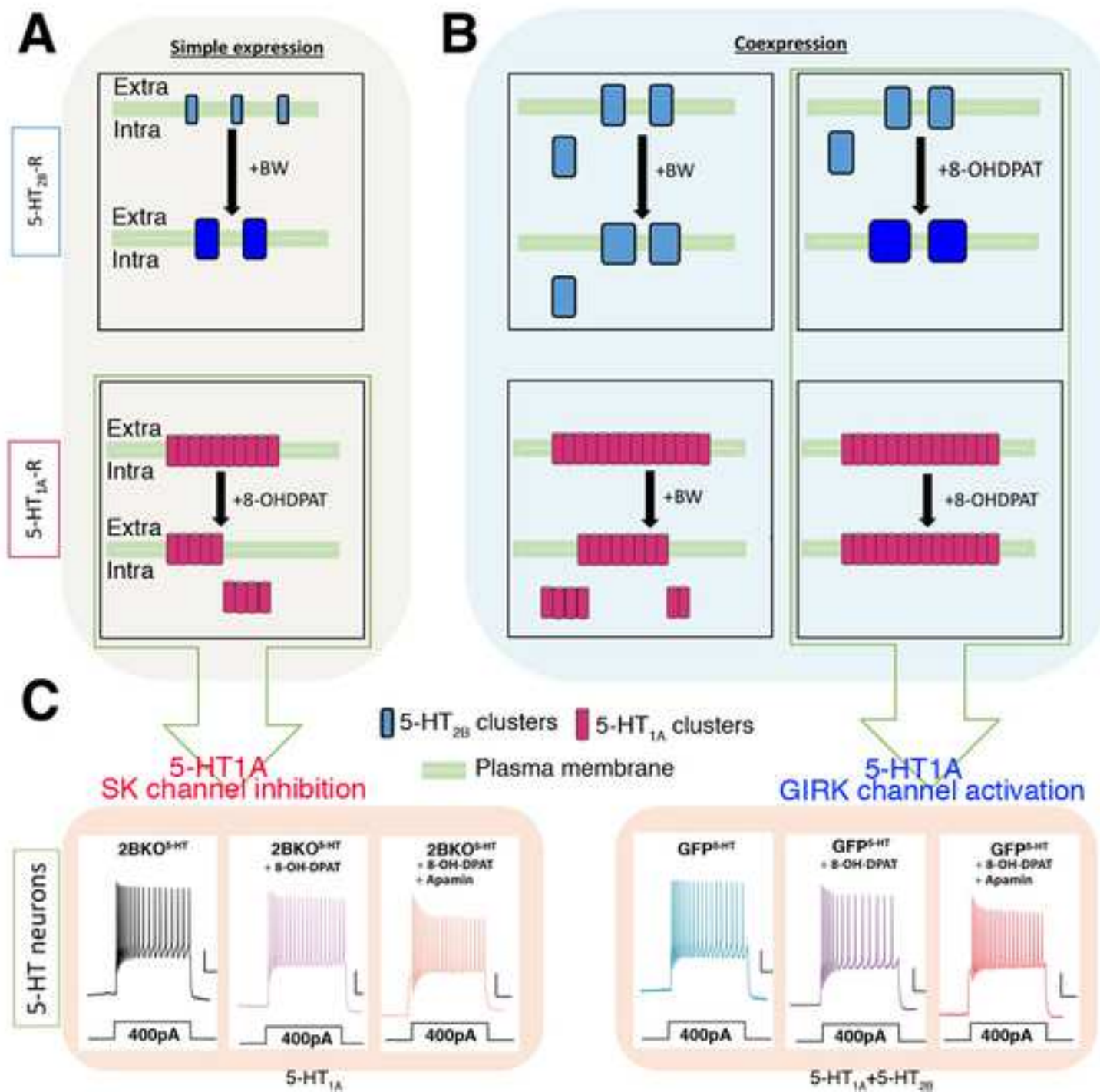


Table S1- Statistics

Full statistical analysis of figure 1 to 7 and Figure S1			
Fig 1. Pharmacology of cells expressing 5-HT _{2B} with or without 5-HT _{1A}			
Fig 1D Mesulergine competition by BW			
Ki values Mann-Whitney unpaired t-test.			P=0.4848
Fig 1F 8-OH-DPAT competition by NAN			
Ki values Mann-Whitney unpaired t-test.			P=0.8857
Fig 1H Inositolphosphate formation upon BW stimulation			
EC50 values Mann-Whitney unpaired t-test.			P=0.2403
Fig2			
Fig 2B Radioligand binding from intact cells expressing 5-HT _{2B} with or without 5-HT _{1A}			
Comparison between Bmax, unpaired t-test with Welch's correction		t7.6=2.587	p=0.0336
Fig 2C-E Surface biotinylation on COS-7 cells expressing 5-HT _{1A} and/or 5-HT _{2B}			
Fig 2D Ratio total vs surface expression for 5-HT _{2B} unpaired t-test			
		t8=2.336	p=0.0477
Fig 2E Ratio total vs surface expression for 5-HT _{1A} unpaired t-test			
		t8=0.9223	p=0.3834
Fig3			
Fig3B Ratio of membrane vs total expression for 5-HT _{2B}			
unpaired t-test		t42=2.765	p=0.0084
Fig3C D 5-HT _{2B} Membrane clusters, BW723C86 stimulation			
Number			
Kruskal-Wallis test		P value	<0.0001
Dunn's multiple comp	Mean rank diff.		Adj P Val
2B t0 number vs. 2B t10 number	42.89		0.0026
2B t0 number vs. 2B t20 number	67.32		<0.0001
2B t0 number vs. 2B+1A t0 number	43.99		0.0014
Area			
Kruskal-Wallis test		P value	<0.0001
2B t0 area vs. 2B t10 area	-44.61		0.0016
2B t0 area vs. 2B t20 area	-57.76		<0.0001
2B t0 area vs. 2B+1A t0 area	-45		0.0008
Integrated Intensity			
Kruskal-Wallis test		P value	<0.0001
2B t0 Integrated Int vs. 2B t20 Integrated Int	-48.01		0.0007
2B t10 Integrated Int vs. 2B t20 Integrated Int	-35.77		0.0421
Fig 3E F 5-HT _{1A} Membrane expression, 8-OH-DPAT stimulation			
Kruskal-Wallis test		P value	<0.0001
Dunn's multiple comp	Mean rank diff.		Adj P Value
1A t0 vs. 1A t10	44.25		0.0115
1A t0 vs. 1A+2B t0	-39.87		0.0172
1A t0 vs. 1A+2B t10	-46.74		0.0069
Fig 4			
Fig 4B STORM 5-HT _{2B} Membrane clusters, BW723C86 stimulation			
Two way ANOVA			
Number			
Interaction		F _{1,70} = 0.9756	P=0.3267
Treatment		F _{1,70} = 11.15	P=0.0014
Transfection		F _{1,70} = 25.31	P<0.0001
Tukey's multiple comp	Mean Diff	95% CI	Adj P Val
t0:5-HT _{2B} vs. t0:5-HT _{2B} +5-HT _{1A}	51.61	19.69 to 83.53	0.0004
t0:5-HT _{2B} vs. t20:5-HT _{2B}	37.1	3.095 to 71.1	0.0271
t0:5-HT _{2B} vs. t20:5-HT _{2B} +5-HT _{1A}	71.77	39.85 to 103.7	<0.0001
t0:5-HT _{2B} +5-HT _{1A} vs. t20:5-HT _{2B}	-14.51	-46.43 to 17.41	0.6311
t0:5-HT _{2B} +5-HT _{1A} vs. t20:5-HT _{2B} +5-HT _{1A}	20.16	-9.522 to 49.84	0.2879
t20:5-HT _{2B} vs. t20:5-HT _{2B} +5-HT _{1A}	34.67	2.754 to 66.59	0.0280
Area			
Interaction		F _{1,70} = 0.0629	P=0.8027
Treatment		F _{1,70} = 7.067	P=0.0097
Transfection		F _{1,70} = 16.78	P=0.0001

Tukey's multiple comp	Mean Diff	95% CI	Adj P Value
t0:5-HT _{2B} vs. t0:5-HT _{2B} +5-HT _{1A}	-191.7	-377.2 to -6.161	0.0402
t0:5-HT _{2B} vs. t20:5-HT _{2B}	-120	-317.6 to 77.65	0.3865
t0:5-HT _{2B} vs. t20:5-HT _{2B} +5-HT _{1A}	-336.7	-522.2 to -151.2	<0.0001
t0:5-HT _{2B} +5-HT _{1A} vs. t20:5-HT _{2B}	71.67	-113.8 to 257.2	0.7402
t0:5-HT _{2B} +5-HT _{1A} vs. t20:5-HT _{2B} +5-HT _{1A}	-145	-317.5 to 27.52	0.1300
t20:5-HT _{2B} vs. t20:5-HT _{2B} +5-HT _{1A}	-216.7	-402.2 to -31.16	0.0156
Fig 5			
Fig 5A 5-HT _{1A} Membrane expression. BW723C86 stimulation			
One way ANOVA	F _{2,43} = 16.15	P value	<0.0001
Tukey's multiple comp	Mean diff.		Adj P Value
5-HT _{1A} t0 vs. 5-HT _{1A} +5-HT _{2B} t0	-27.87		0.0188
5-HT _{1A} t0 vs. 5-HT _{1A} +5-HT _{2B} t20"	27.35		0.0463
5-HT _{1A} +5-HT _{2B} t0 vs. 5-HT _{1A} +5-HT _{2B} t20"	55.22		<0.0001
Fig 5B 5-HT _{2B} Membrane expression. 8-OH-DPAT stimulation			
Number			
Kruskal-Wallis test		P value	<0.0001
Dunn's multiple comp	Mean rank		Adj P Value
2B+1A t0 nb vs. 2B+1A t10 nb	25.33		<0.0001
2B+1A t0 nb vs. 2B+1A t20 nb	20.93		0.0001
Area			
Kruskal-Wallis test		P value	<0.0001
2B+1A t0 area vs. 2B+1A t10 area	-27.52		<0.0001
2B+1A t0 area vs. 2B+1A t20 area	-21.82		<0.0001
Integrated intensity			
Kruskal-Wallis test		P value	<0.0001
2B+1A t0 Integrated Intensity vs. 2B+1A t10 II	-27.11		<0.0001
2B+1A t0 II vs. 2B+1A t20 II	-23.13		<0.0001
Fig 6			
Fig 6A 5-HT _{2B} Membrane expression. 5-HT stimulation			
Number			
Kruskal-Wallis test		P value	<0.0001
Dunn's multiple comp	Mean rank		Adj P Value
2B t0 nbr vs. 2B+1A t0 nbr	40.63		<0.0001
2B t0 nbr vs. 2B+1A t20 nbr	60.67		<0.0001
2B t20 nbr vs. 2B+1A t20 nbr	67.58		<0.0001
Area			
Kruskal-Wallis test		P value	<0.0001
2B t0 area vs. 2B+1A t0 area	-43.91		<0.0001
2B t0 area vs. 2B+1A t20 area	-61.21		<0.0001
2B t20 area vs. 2B+1A t20 area	-66.09		<0.0001
Kruskal-Wallis test		P value	0.2387
Fig 6 C 5-HT _{1A} Membrane expression. 5-HT stimulation			
Kruskal-Wallis test		P value	<0.0001
Dunn's multiple comp		Mean rank	Adj P Value
1A t0 vs. 1A t20		50.2	0.0003
1A t0 vs. 2B+1A t20		48.18	0.0014
2B+1A t0 vs. 2B+1A t20		76.51	<0.0001
2B+1A t20 vs. 2B+1A t20+RS		-49.73	0.0023
Fig 7			
Fig 7C Firing rate GFP ^{5-HT} vs. 2B-KO ^{5-HT} ::GFP ^{5-HT}			
Two way ANOVA-Repeated measure			
Interaction		F _{13, 663} = 0.2221	P=0.9983
Depolarization		F _{13, 663} = 400.3	P<0.0001
Genotype		F _{1, 51} = 0.0353	P=0.8517

Fig 7D			
Resting membrane potential values GFP ^{5-HT} vs. 2B-KO ^{5-HT} ::GFP ^{5-HT}			
Mann-Whitney unpaired t-test.		P=0.1820	
Input resistance values GFP ^{5-HT} vs. 2B-KO ^{5-HT} ::GFP ^{5-HT}			
Mann-Whitney unpaired t-test.		P=0.8255	
Fig 7E			
Firing rate GFP ^{5-HT} vs. 2B-KO ^{5-HT} ::GFP ^{5-HT} in the presence of 8-OH-DPAT;			
Two way ANOVA-Repeated measure			
Interaction		F _{13,806} = 8.011	P<0.0001
Depolarization		F _{13,806} = 536.6	P<0.0001
Genotype		F _{1,62} = 23.74	P<0.0001
Sidak's multiple comp			
	Mean Diff	95% CI	Adj P Val
200pA	-6.567	-12.74 to -0.3976	0.0274
250pA	-7.907	-14.08 to -1.738	0.0028
300pA	-9.466	-15.64 to -3.296	0.0001
350pA	-10.12	-16.29 to -3.948	<0.0001
400pA	-10.77	-16.94 to -4.601	<0.0001
450pA	-10.98	-17.15 to -4.813	<0.0001
500pA	-11.18	-17.35 to -5.014	<0.0001
550pA	-12.05	-18.22 to -5.881	<0.0001
600pA	-11.2	-17.37 to -5.026	<0.0001
650pA	-11.28	-17.45 to -5.107	<0.0001
Fig 7F			
Resting membrane potential values GFP ^{5-HT} vs. 2B-KO ^{5-HT} ::GFP ^{5-HT} in the presence of 8-OH-DPAT			
Mann-Whitney unpaired t-test.			P=0.3588
Input resistance values GFP ^{5-HT} vs. 2B-KO ^{5-HT} ::GFP ^{5-HT} in the presence of 8-OH-DPAT			
Mann-Whitney unpaired t-test.			P=0.6269
Fig 7G			
Firing rate GFP ^{5-HT} vs. 2B-KO ^{5-HT} ::GFP ^{5-HT} in the presence of 8-OH-DPAT+Apamin;			
Two way ANOVA-Repeated measure			
Interaction		F _{9,504} = 0.7975	P=0.6188
Depolarization		F _{9,504} = 329	P<0.0001
Genotype		F _{1,56} = 0.1706	P=0.6811
Fig 7H			
Resting membrane potential values GFP ^{5-HT} vs. 2B-KO ^{5-HT} ::GFP ^{5-HT} in the presence of 8-OH-DPAT+Apamin			
Mann-Whitney unpaired t-test.			P=0.6668
Input resistance values GFP ^{5-HT} vs. 2B-KO ^{5-HT} ::GFP ^{5-HT} in the presence of 8-OH-DPAT+Apamin			
Mann-Whitney unpaired t-test.			P=0.1196
FigS1			
Resting membrane potential GFP ^{5-HT} vs. 2B-KO ^{5-HT} ::GFP ^{5-HT} effect of 8-OHDPAT			
Two way ANOVA			
Interaction		F _{1,113} = 3.186	P=0.0769
Treatment		F _{1,113} = 115.7	P<0.0001
Genotype		F _{1,113} = 0.0538	P=0.8170
Tukey's multiple comp			
	Mean Diff	95% CI	Adj P Val
GFP ^{5-HT} saline vs. GFP ^{5-HT} 8-OHDPAT	9.629	5.736 to 13.52	<0.0001
2B-KO ^{5-HT} saline vs. vs. 2B-KO ^{5-HT} 8-OHDPAT	13.46	9.439 to 17.48	<0.0001
Input resistance GFP ^{5-HT} vs. 2B-KO ^{5-HT} ::GFP ^{5-HT} effect of 8-OH-DPAT			
Two way ANOVA			
Interaction		F _{1,113} = 0.3622	P=0.5485
treatment		F _{1,113} = 121.7	P<0.0001
Genotype		F _{1,113} = 0.0724	P=0.7884
Tukey's multiple comp			
	Mean Diff	95% CI	Adj P Val
GFP ^{5-HT} saline vs. GFP ^{5-HT} 8-OHDPAT	443.9	305.5 to 582.3	<0.0001
2B-KO ^{5-HT} saline vs. vs. 2B-KO ^{5-HT} 8-OHDPAT	398	255 to 540.9	<0.0001

Supplementary data and material

Figure S1

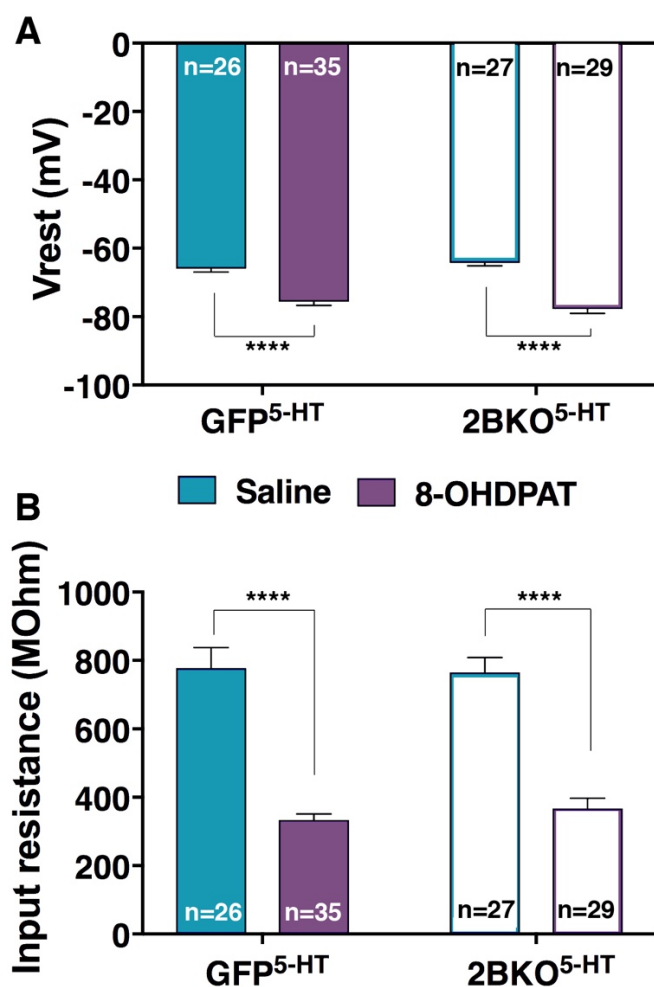


Figure S1 related to figure 7: Effect of 5-HT_{1A} stimulation by 8-OHDPAT on electrophysiological properties of 5-HT neurons from GFP^{5-HT} and 2B-KO^{5-HT}::GFP^{5-HT} mice related to figure 7. (A) Resting membrane potential. The resting membrane potential of GFP^{5-HT} and 2B-KO^{5-HT}::GFP^{5-HT} was significantly decreased by 8-OHDPAT (30 nM). Two-way ANOVA revealed an effect of 8-OHDPAT treatment $F_{1, 113} = 115.7$ $P < 0.0001$ (**); 8-OHDPAT-treated GFP^{5-HT} vs. 8-OHDPAT-treated 2B-KO^{5-HT}::GFP^{5-HT} mice, $p < 0.0001$ (****) by Tukey's multiple comparisons test. (B) Input resistance. The input resistance GFP^{5-HT} and 2B-KO^{5-HT}::GFP^{5-HT} was significantly decreased by 8-OHDPAT (30 nM). Two-way ANOVA revealed only an effect of 8-OHDPAT treatment $F_{1, 113} = 121.7$, $P < 0.0001$; 8-OHDPAT-treated GFP^{5-HT} vs. GFP^{5-HT} $p < 0.0001$ (****); 8-OHDPAT-treated 2B-KO^{5-HT}::GFP^{5-HT} vs. 2B-KO^{5-HT}::GFP^{5-HT} mice, $p < 0.0001$ (****) by Tukey's multiple comparisons test. $n = 26-35$ and $27-29$ neurons, 1-2 neurons per slice, 3-4 slice from 3-6 mice. Error bars represent mean \pm SEM.**

Figure S2: Maps of the AAV-DIO-HA-5-HT_{2B} and AAV-DIO-FLAG-5-HT_{1A} viruses

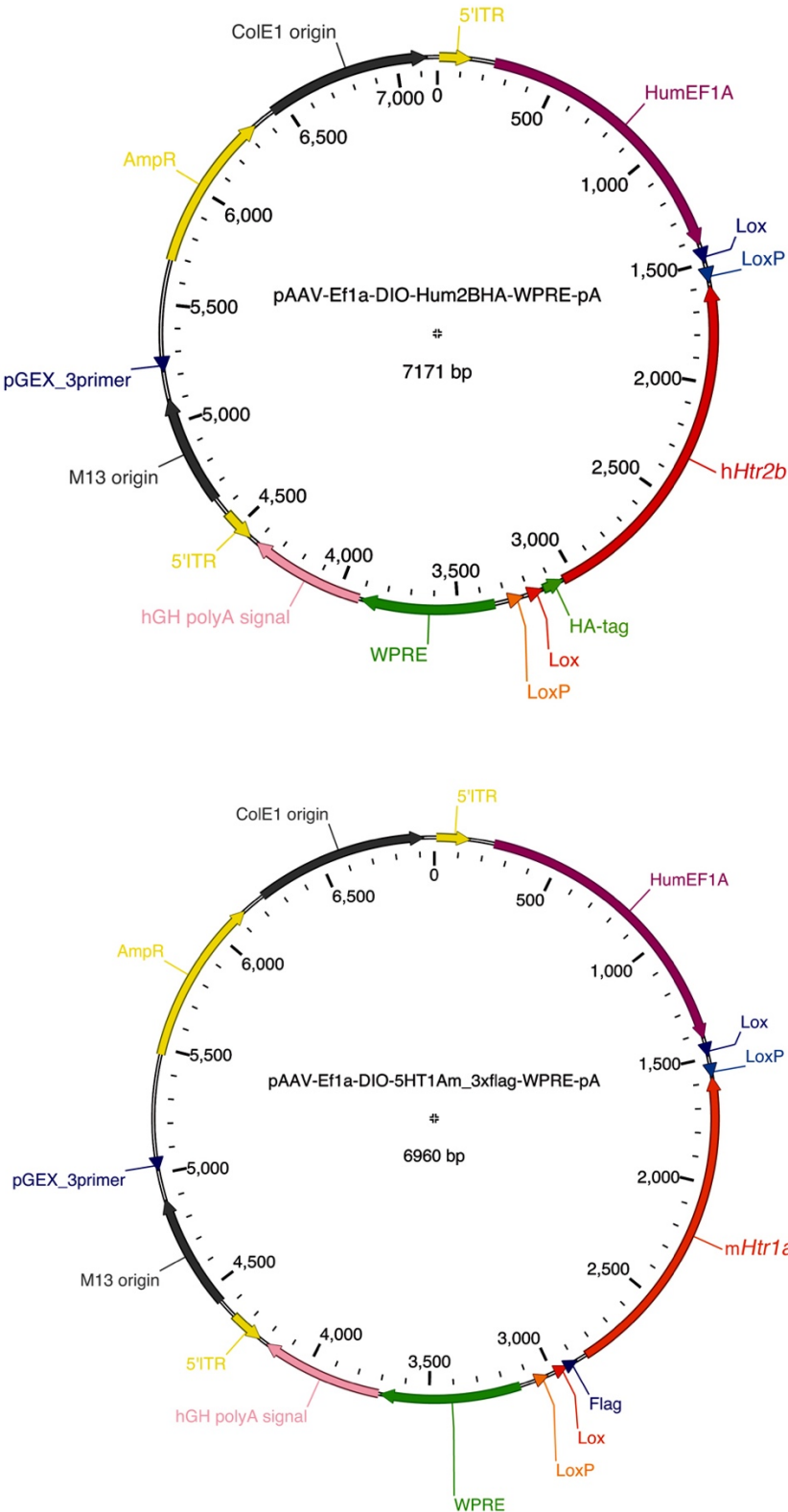


Figure S2: Maps of the AAV-DIO-HA-5-HT_{2B} and AAV-DIO-FLAG-5-HT_{1A} viruses related to methods details, viral constructs and stereotaxic injections. (Top) Map of pAAV-Ef1a-DIO-HA-5-HT_{2B}. (Bottom) Map of pAAV-Ef1a-DIO-Flag-5-HT_{1A}.

Table S2 ARRIVE

Item	Recommendation	Section
Study design 1	a. The groups being compared, including control groups. If no control group has been used, the rationale should be stated.	Experimental model, Table S1
	b. The experimental unit (e.g., a single animal, litter, or cage of animals).	Method details
Sample size 2	a. Specify the exact number of experimental units allocated to each group, and the total number in each experiment. Also indicate the total number of animals used.	Quantification and statistical analysis, Table S1
	b. Explain how the sample size was decided. Provide details of any a priori sample size calculation, if done.	Method details
Inclusion and exclusion criteria 3	a. Describe any criteria used for including and excluding animals (or experimental units) during the experiment, and data points during the analysis. Specify if these criteria were established a priori. If no criteria were set, state this explicitly.	Quantification and statistical analysis, Table S1
	b. For each experimental group, report any animals, experimental units, or data points not included in the analysis and explain why. If there were no exclusions, state so.	Quantification and statistical analysis, Table S1
	c. For each analysis, report the exact value of n in each experimental group.	Figure captions,
Randomisation 4	a. State whether randomisation was used to allocate experimental units to control and treatment groups. If done, provide the method used to generate the randomisation sequence.	Method details
	b. Describe the strategy used to minimise potential confounders such as the order of treatments and measurements, or animal/cage location. If confounders were not controlled, state this explicitly.	Method details

Blinding 5	Describe who was aware of the group allocation at the different stages of the experiment (during the allocation, the conduct of the experiment, the outcome assessment, and the data analysis).	Method details
Outcome measures 6	a. Clearly define all outcome measures assessed (e.g., cell death, molecular markers, or behavioural changes).	Method details
	b. For hypothesis-testing studies, specify the primary outcome measure, i.e., the outcome measure that was used to determine the sample size.	Method details, Quantification and statistical analysis, Table S1
Statistical methods 7	a. Provide details of the statistical methods used for each analysis, including software used.	Quantification and statistical analysis, Table S1
	b. Describe any methods used to assess whether the data met the assumptions of the statistical approach, and what was done if the assumptions were not met.	Quantification and statistical analysis, Table S1
Experimental animals 8	a. Provide species-appropriate details of the animals used, including species, strain and substrain, sex, age or developmental stage, and, if relevant, weight.	Experimental model,
	b. Provide further relevant information on the provenance of animals, health/immune status, genetic modification status, genotype, and any previous procedures.	Experimental model,
Experimental procedures 9	a. What was done, how it was done, and what was used.	STAR*Methods, Method details
	b. When and how often.	STAR*Methods, Method details
	c. Where (including detail of any acclimatisation periods).	Experimental model,
	d. Why (provide rationale for procedures).	Experimental model,
Results 10	a. Summary/descriptive statistics for each experimental group, with a measure of variability where applicable (e.g., mean and SD, or median and range).	Results, Table S1, Figure captions
	b. If applicable, the effect size with a confidence interval.	Table S1

CELL PRESS DECLARATION OF INTERESTS POLICY

Transparency is essential for a reader's trust in the scientific process and for the credibility of published articles. At Cell Press, we feel that disclosure of competing interests is a critical aspect of transparency. Therefore, we require a "declaration of interests" section in which all authors disclose any financial or other interests related to the submitted work that (1) could affect or have the perception of affecting the author's objectivity or (2) could influence or have the perception of influencing the content of the article.

What types of articles does this apply to?

We require that you disclose competing interests for all submitted content by completing and submitting the form below. We also require that you include a "declaration of interests" section in the text of all articles even if there are no interests to declare.

What should I disclose?

We require that you and all authors disclose any personal financial interests (e.g., stocks or shares in companies with interests related to the submitted work or consulting fees from companies that could have interests related to the work), professional affiliations, advisory positions, board memberships (including membership on a journal's advisory board when publishing in that journal), or patent holdings that are related to the subject matter of the contribution. As a guideline, you need to declare an interest for (1) any affiliation associated with a payment or financial benefit exceeding \$10,000 p.a. or 5% ownership of a company or (2) research funding by a company with related interests. You do not need to disclose diversified mutual funds, 401ks, or investment trusts.

Authors should also disclose relevant financial interests of immediate family members. Cell Press uses the Public Health Service definition of "immediate family member," which includes spouse and dependent children.

Where do I declare competing interests?

Competing interests should be disclosed on this form as well as in a "declaration of interests" section in the manuscript. This section should include financial or other competing interests as well as affiliations that are not included in the author list. Examples of "declaration of interests" language include:

"AUTHOR is an employee and shareholder of COMPANY."

"AUTHOR is a founder of COMPANY and a member of its scientific advisory board."

NOTE: Primary affiliations should be included with the author list and do not need to be included in the "declaration of interests" section. Funding sources should be included in the "acknowledgments" section and also do not need to be included in the "declaration of interests" section. (A small number of front-matter article types do not include an "acknowledgments" section. For these articles, reporting of funding sources is not required.)

What if there are no competing interests to declare?

If you have no competing interests to declare, please note that in the "declaration of interests" section with the following wording:

"The authors declare no competing interests."

CELL PRESS DECLARATION OF INTERESTS FORM

If submitting materials via Editorial Manager, please complete this form and upload with your initial submission. Otherwise, please email as an attachment to the editor handling your manuscript.

Please complete each section of the form and insert any necessary “declaration of interests” statement in the text box at the end of the form. A matching statement should be included in a “declaration of interests” section in the manuscript.

Institutional affiliations

We require that you list the current institutional affiliations of all authors, including academic, corporate, and industrial, on the title page of the manuscript. ***Please select one of the following:***

- All affiliations are listed on the title page of the manuscript.
- I or other authors have additional affiliations that we have noted in the “declaration of interests” section of the manuscript and on this form below.

Funding sources

We require that you disclose all funding sources for the research described in this work. ***Please confirm the following:***

- All funding sources for this study are listed in the “acknowledgments” section of the manuscript.*

*A small number of front-matter article types do not include an “acknowledgments” section. For these, reporting funding sources is not required.

Competing financial interests

We require that authors disclose any financial interests and any such interests of immediate family members, including financial holdings, professional affiliations, advisory positions, board memberships, receipt of consulting fees, etc., that:

- (1) could affect or have the perception of affecting the author’s objectivity, *or*
- (2) could influence or have the perception of influencing the content of the article.

Please select one of the following:

- We, the authors and our immediate family members, have no financial interests to declare.
- We, the authors, have noted any financial interests in the “declaration of interests” section of the manuscript and on this form below, and we have noted interests of our immediate family members.

Advisory/management and consulting positions

We require that authors disclose any position, be it a member of a board or advisory committee or a paid consultant, that they have been involved with that is related to this study. We also require that members of our journal advisory boards disclose their position when publishing in that journal. **Please select one of the following:**

- We, the authors and our immediate family members, have no positions to declare and are not members of the journal's advisory board.
- The authors and/or their immediate family members have management/advisory or consulting relationships noted in the "declaration of interests" section of the manuscript and on this form below.

Patents

We require that you disclose any patents related to this work by any of the authors or their institutions. **Please select one of the following:**

- We, the authors and our immediate family members, have no related patents to declare.
- We, the authors, have a patent related to this work, which is noted in the "declaration of interests" section of the manuscript and on this form below, and we have noted the patents of immediate family members.

Please insert any "declaration of interests" statements in this space. This exact text should also be included in the "declaration of interests" section of the manuscript. If no authors have a competing interest, please insert the text, "The authors declare no competing interests."

The authors declare no conflict of interest.

On behalf of all authors, I declare that I have disclosed all competing interests related to this work. If any exist, they have been included in the "declaration of interests" section of the manuscript.

Name:

Maroteaux Luc

Manuscript
number
(if available):

ISCIENCE-D-23-01784